Available online at www.sciencedirect.com
ScienceDirect
Icarus 189 (2007) 308–324
ICARUS
www.elsevier.com/locate/icarus

Exploration of hydrothermal targets on Mars

Dirk Schulze-Makuch [a,*], James M. Dohm [b,c], Chaojun Fan [a], Alberto G. Fairén [d,e], J.A.P. Rodriguez [f], Victor R. Baker [b,c], Wolfgang Fink [g]

[a] *School of Earth and Environmental Sciences, Washington State University, Pullman, WA 99164, USA*
[b] *Department of Hydrology and Water Resources, University of Arizona, Tucson, AZ 85721, USA*
[c] *Lunar and Planetary Laboratory, University of Arizona, 1629E. University Blvd., Tucson, AZ 85721, USA*
[d] *Space Science and Astrobiology Division, NASA Ames Research Center, Moffett Field, 94035 CA, USA*
[e] *Centro de Biología Molecular, CSIC-Universidad Autónoma de Madrid, 28049-Cantoblanco, Madrid, Spain*
[f] *Planetary Science Institute, 1700E. Fort Lowell Rd., Tucson, AZ 85719, USA*
[g] *Visual and Autonomous Exploration Systems Research Laboratory, Division of Physics, Mathematics and Astronomy, California Institute of Technology, Pasadena, CA 91125, USA*

Received 28 April 2006; revised 31 January 2007

Available online 7 March 2007

Abstract

Based on various lines of geologic, geomorphic, topographic, geophysical, spectral, and elemental evidence, we conclude that hydrothermal environments have certainly existed on Mars and are likely to still exist. Here, we present candidate targets of endogenic- and exogenic-driven hydrothermal environments on Mars based on a set of selection criteria and suggest strategies for the detection of such targets. This includes a re-evaluation of potential targets using both existing and yet-to-be-released remote information provided by the instruments onboard the Mars orbiters and rovers. We also provide terrestrial analogs for possible martian hydrothermal environments to highlight the implications of these targets for potential martian life. This compilation and synthesis of data from martian localities indicating hydrothermal activity is timely and a first step towards prioritizing candidate targets for further investigation, which will likely add more targets to this list. Future in situ exploration will have to focus on the most promising of the hydrothermal targets and investigate them utilizing a novel integrated multi-tier, multi-agent reconnaissance mission architecture.

Keywords: Mars; Thermal histories; Cratering; Exobiology; Astrobiology

1. Introduction

Geomorphic features, such as valley networks, large outflow channels, sapping channels, valleys and associated alluvial fans, and other valley forms of diverse geometric shapes and varying ages indicate that water-related processes have played a significant role in the modification of the martian surface during the geologic past. Past and present water enrichment for parts of Mars is further supported by spectral (e.g., Christensen et al., 2001; Rieder et al., 2004; Herkenhoff et al., 2004; Bibring et al., 2006) and elemental (Boynton et al., 2002; Feldman et al., 2002) information. Hydrothermal activity was likely more common and widespread during the early geologic history of Mars, as indicated by: (1) the extensive Noachian terrains, interpreted in many cases to be igneous in composition (Scott and Tanaka, 1986; Greeley and Guest, 1987; Tanaka, 1986); (2) evidence for a significant volatile inventory during the Noachian (e.g., Clifford and Parker, 2001; Fairén et al., 2003); and (3) the large amounts of heat released by both endogenic activity during the embryonic stages of planetary evolution (Schubert et al., 1992) and cosmic impacts (exogenic activity) during a hypothesized spiked period of impact catastrophism (Strom et al., 2005).

If life developed on Mars, it may have left behind a fossil record at hydrothermal environments due to suitable preservation conditions combined with an abundance of long-term energy sources and water. Alternatively, extant life may still be

* Corresponding author.
E-mail address: dirksm@wsu.edu (D. Schulze-Makuch).

0019-1035/$ – see front matter
doi:10.1016/j.icarus.2007.02.007

present at moderate depths in the subsurface. Small, single-cell prokaryotes were vitally important in the evolution of Earth and these microorganisms are exquisitely adapted to environmental extremes of pH, temperature, salinity, and anoxic conditions (e.g., Schulze-Makuch and Irwin, 2004). The identification of hydrothermal environments at local to regional scales on Mars has been researched by many authors, including Carr (1979), Newsom (1980), Mouginis-Mark (1985, 1990), Brakenridge et al. (1985), Squyres et al. (1987), McKay and Stoker (1989), Gulick and Baker (1990), MacKinnon and Tanaka (1989), Gulick (1993), Clifford (1993), Greeley and Thomas (1994), Carr (1995), Gulick et al. (1997), Wilson and Head (1997), Tanaka et al. (1998), and Dohm et al. (1998a, 2000, 2001a, 2001b, 2001c, 2004). These environments will likely remain a research focus in the future, since many are (1) favorable targets for the development and sustenance of extant life, (2) may comprise a large variety of exotic mineral assemblages, and (3) could potentially contain water reservoirs for future Mars-related human activities.

2. Martian hydrothermal environments

Recorded geologic activity coupled with extensive evidence of past and present-day water/ice, above and below the martian surface, indicate that hydrothermal environments certainly existed in the past and may still exist today. Confidence in identifying such environments at the martian surface is based on distinct geologic, paleohydrologic, paleotectonic, topographic, geophysical, spectral, and elemental signatures. The presented list of targeted environments of endogenic- and exogenic-driven hydrothermal activity is not a final list, but rather a first attempt of compiling candidate hydrothermal targets, which appear especially promising based on a set of selection criteria. The selection criteria include: (1) geomorphologic evidence of the action of liquid water; (2) stratigraphic and geomorphologic evidence of volcanic constructs and/or lava flows; (3) stratigraphic and paleotectonic evidence for a center of magmatic-driven tectonism (e.g., see Anderson et al., 2001, 2004); (4) topographic depressions and/or valleys hypothesized to be the result of structurally controlled collapse and/or rifting, respectively, based on stratigraphic, geomorphic, topographic, and paleotectonic evidence; (5) geomorphologic evidence of impact craters in ice-rich regions; (6) identification of deposits usually associated with hydrothermal activity, such as carbonates, sulfates and sulfides, and metal hydroxides/oxides; (7) identification of deposits indicative of water alterations such as hydrated phyllosilicates, the minerals jarosite and hematite, or Gamma Ray Spectrometer (GRS)-based elevated elements such as chlorine; and (8) geological similarities to hydrothermal analog environments on Earth. These selection criteria are based on current knowledge and instrumental abilities. As more spacecrafts arrive at Mars with more sophisticated instrumentation other selection criteria should be added. An example would be (9) spectroscopic evidence for increased heat flow, especially in ice-rich regions. However, this capability and the required resolution may not be currently available, as there has yet to be identification of such environments through thermal IR or otherwise. Also, it should be pointed out that we likely missed many of the selection criteria at prospective locations due to obscuration by factors including atmospheric conditions at the time of data acquisition, wind-, water-, and gravity-driven processes (e.g., mantling of evidence by eolian, fluvial, alluvial, and colluvial deposits), and spatial association with respect to the surface (e.g., subterranean caves may exist but go unnoticed without the aid of geophysical data and/or surface expression such as noted in Rodriguez et al., 2005a, 2005b). Thus, a lack of detection at the present time does not necessarily imply that it does not exist. Several prominent candidate targets of endogenic- and exogenic-associated hydrothermal activity are discussed below and shown in Figs. 1 and 2 and corresponding Tables 1 and 2.

2.1. Endogenic-driven activity and associated candidate hydrothermal environments

Endogenic activity on Mars has been manifested as large-scale, tectono-magmatic complexes, Tharsis and Elysium (Komatsu et al., 2004a, 2004b), and to a lesser extent, as volcanic provinces that have formed along impact-induced basement structures. These include the southern (Malea Planum; e.g., Tanaka and Scott, 1987; Tanaka et al., 1992) and northeastern (Tyrrehena and Hadriaca Paterae; e.g., Crown et al., 1992) margins of the primary Hellas basin, and the western margin of the Isidis impact basin (Syrtis Major; e.g., Greeley and Guest, 1987). Similar to parts of Tharsis, which record magma–water interactions (e.g., Mouginis-Mark, 1990; Tanaka et al., 1998), the geologic, geomorphic, topographic, and elemental evidence indicate that Malea Planum and surrounding regions may also reflect such activity, including windblown deposition of the resulting altered rock materials at regional scales (Scott et al., 1995; Moore and Wilhems, 2001; Tanaka et al., 2002; Taylor et al., 2006).

In particular, the Tharsis complex is comprised of a diverse suite of characteristics including: (1) ancient mountain ranges; (2) distinct episodes of intensive early magmatic/tectonic activity that declines with time and related hydrologic activity; (3) a Europe-sized ($\sim 10^7$ km^2) drainage basin in the eastern part of the complex; (4) local and regional centers of magmatic-driven uplift and associated tectonism, dike emplacement, volcanism, and possible fluvial and hydrothermal activity; (5) large igneous plateaus; (6) gigantic outflow channel systems, all of which source from chaotic terrain or fracture systems; (7) circumferential systems of wrinkle ridges and fold belts; (8) volcanic constructs of diverse sizes and shapes and extensive lava flow fields; (9) putative ash-flow and air-fall deposits; (10) valley forms of diverse geometric shapes, origins, and relative age of formation; and (11) fracture, fault, rift, pit crater chain, and canyon systems of varying extent and relative age of formation (Dohm et al., 2001a, 2002a). Twenty of the listed candidate targets in Tables 1 and 2 are associated with the Tharsis tectono-magmatic complex and thus underline the importance of this region. A point to be addressed for Tharsis and other locations is the distinction between purely tectonically driven resurfacing and resurfacing driven by magmatic heat release, a distinction which is difficult to make given

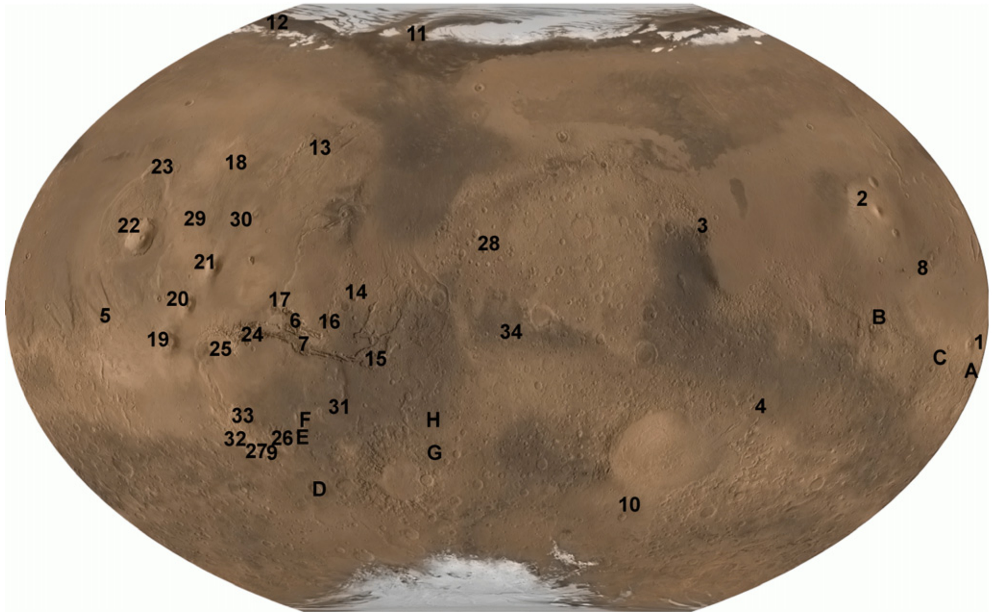

Fig. 1. MOLA- and MOC-based map of Mars showing the location of candidate targets of endogenic-driven hydrothermal activity. Numbers 1–29 correspond to those in Tables 1 and 2. Note that the locations of Gusev (A), Gale (B), Boeddicker (C), Lowell (D), Lampland (E), Voeykov (F), Hale (G), and Bond (H) impact craters are also shown (Image credit: National Geographic Society, MOLA Science Team, MSS, JPL, NASA.)

the current data. With this point in mind, several of the candidate targets of hydrothermal activity have been identified as centers of tectonism through the compilation of a paleotectonic map of the western equatorial region of Mars and by performing analysis of the spatial and temporal tectonic data through the Vector Analysis (VA) method (Anderson et al., 2001). These centers, which were later determined to be distinct topographic highs through subsequent Mars Orbiter Laser Altimeter (MOLA) data, were interpreted to be manifestations of magmatic-driven activity, including uplift, dike emplacement, volcanism, and possible hydrothermal activity (Anderson et al., 2001; Dohm et al., 2001a). A prime example is the central part of Valles Marineris where magmatic-driven uplift was hypothesized to explain the strain history documented using Viking data, later identified to be a distinct topographic rise in the MOLA data (Dohm et al., 1998b, 2001a, 2001b, 2001c). Other evidence for magmatism associated with the geologic history of Valles Marineris are presented in numerous works (e.g., Lucchitta et al., 1992; Chapman and Tanaka, 2001; Komatsu et al., 2004a, 2004b).

Plumes are an integral part of the internal dynamics of terrestrial planets, having profound influences on surface and subsurface geology and hydrology over long time scales (Komatsu et al., 2004a, 2004b). They can significantly alter large-scale topography, drainages, landscapes, sedimentation, climate (Baker et al., 1991; Maruyama, 1994), and even break up a continent (Li et al., 2003). In the case of Tharsis, which is estimated to have evolved for more than 3.5 Ga, catastrophic release of endogenic activity is observed for at least five pronounced stages based on a synthesis of geologic information (Dohm et al., 1998a, 2001a, 2001b, 2001c). Several processes have been involved: (1) magmatism, tectonism, and hydrogeologic activity, which includes emplacement of lava flows; (2) the triggering of tremendous outburst flooding that contributed to the formation of the circum-Chryse outflow channels and associated chaotic terrain that mark the channels' source regions and the Northwestern Slope Valleys (NSVs); (3) ponding of floodwaters in the northern plains to form at least transient bodies of water ranging from lakes to oceans; (4) climatic perturbations; and (5) a transient dynamic unvegetated martian landscape (e.g., Fairén et al., 2003). Assuming the availability of water in the region where the magmatic–tectonic activity is occurring, hydrothermal activity is expected to be pronounced during the distinct heightened stages of endogenic-induced activity. Also, spring-fed fluvial activity along breaks in slopes such as along the highland–lowland boundary support this notion (Tanaka et al., 2003, 2005).

A hypothesized major water source for the NSVs and the circum-Chryse outflow channel systems is a Noachian Europe-sized drainage basin/aquifer system that has been unfolded through paleotopographic reconstructions of the major stages of Tharsis evolution (Dohm et al., 2001a, 2001c). This system has Valles Marineris as its central part and ancient Thaumasia highlands and Coprates rise mountain ranges, highly degraded Chryse impact basin, Tempe igneous plateau, and Ceraunius and Claritas rises as its southern, eastern, northeastern, northwestern, and southwestern margins, respectively. Coupled with the ancient mountain ranges, a circumferential system of fold belts centered about Syria Planum (Schultz and Tanaka, 1994) may have formed aquitards for the movement of groundwater to the south away from the basin/aquifer system, except along extended terrains such as the complex rift system, which sources a system of networking troughs that occur along the southeastern margin of the Thaumasia plateau (Dohm et al., 2001b). Subterranean cavernous systems, including buried impact craters and fracture networks, are hypothesized to have increased hy-

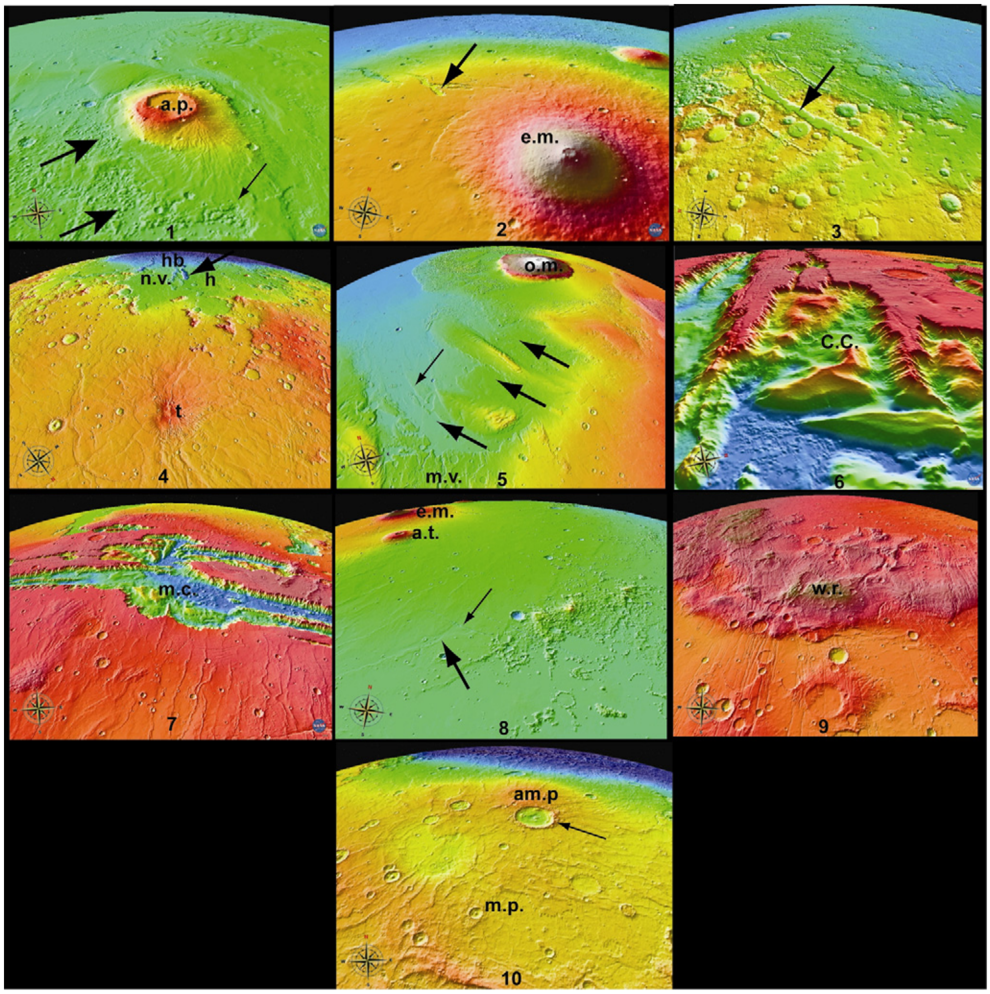

Fig. 2. MOLA-based images of candidate hydrothermal targets; (1) Apollinaris Patera (a.p.) is a seemingly isolated prominent shield volcano spanning about 180 km across at its base. Parts of the shield volcano broke away to contribute to the formation of the chaotic terrain (broad arrows) and a system of channels that source at the southern margin of a late Hesperian lava flow (narrow arrow); (2) Elysium Mons (e.m.) of the Elysium rise volcanic province and a structural feature of Elysium Fossae may point to magmatic/tectonic/aqueous interactions (arrow); the prominent summit caldera is nearly 17 km in diameter; (3) Nili Fossae, a structurally-controlled center of magmatic-driven activity with a central graben nearly 37 km wide; (4) structurally-controlled Hadriaca/Tyrrhena volcanic province, located on the northeast margin of the Hellas impact basin (hb), includes shield volcanoes, Tyrrhena (t) and Hadriaca (h) Paterae, lava flow fields, and outflow channels such as Niger Vallis (n.v.); a valley of Niger Vallis is nearly 50 km wide (arrow); (5) Northwestern Slope Valleys (NSVs) with Olympus Mons (o.m.), the distinct outflow channel system, Mangala Valles (m.v.), the 3 gargantuan valleys (broad arrows) of the NSVs system, each of which are over 200 km wide, and an erosional scarp inset within the southwestern-most valley, indicating aqueous activity (narrow arrow); (6) an east-trending trough of the Valles Marineris canyon system, Candor Chasma (c.c.), comprising canyons, grabens, pit craters, and channels. The canyon is as wide as 130 km in places; (7) the central part of Valles Marineris including Melas Chasma (m.c.), which is more than 280 km across; (8) Cerberus Fossae (narrow arrow) and genetically linked Athabasca Valles (broad arrow). Albor Tholus (a.t.) and Elysium Mons (e.m.) in the background with Albor Tholus nearly 150 km across; (9) Warrego rise within the Noachian Thaumasia highlands mountain range, as much as 130 km across; (10) volcanic province, Malea Planum, partly infills an ancient paleovalley over 1300 km wide, which includes shield volcanoes such as Amphitrites Patera (am.p.), lava flow fields, and valleys. The impact crater Barnard (arrow) is nearly 130 km across.

draulic conductivity and contributed to outflow channel formation (Rodriguez et al., 2005a, 2005b).

Mars may be similar to Earth, where crustal basement structures act as conduits for the lateral and vertical migration of groundwater and other volatiles in the subsurface, and the release of water onto the surface. Such hydrogeologic activity may be enhanced by endogenic heating, for example, by an elevated geothermal gradient or a magma body. On Mars, the spatial and temporal associations among volcanoes, rifts, and channels may indicate the presence of shallow crustal intrusions that could lead to local hydrothermal circulation, melting of ground ice and snow, and groundwater sapping (e.g., southern margin of the Thaumasia plateau; Tanaka et al., 1998). Gulick (1998) demonstrated that systems associated with magmatic intrusions greater than several hundred km^3 in volume can provide sufficient groundwater outflow to form the observed fluvial valleys.

Magma/water interactions have also been documented for both Hadriaca and Tyrrehena Paterae; these two prominent shield volcanoes located near the northeastern margin of the Hellas impact basin were episodically constructed at least during the Noachian and Hesperian periods, and possibly into the Early Amazonian epoch (e.g., Crown et al., 1992; Crown and Greeley, 1993). As such, hydrothermal activity is suspected

Table 1
Top ten candidate targets of endogenic-driven hydrothermal activity on Mars based on total number of selection criteria listed in Section 2

#	Name (for location, see Fig. 1, MOLA-based images shown in Fig. 2)	Relative age and selection criteria based on current knowledge	Description/interpretation
1	Apollinaris Patera	Late Noachian–early Amazonian, and possibly younger activity {1,2,3,4,5,7,8}	Shield volcano, chaotic terrain, valleys, channels, and elevated chlorine (Dohm et al., 2006). Prominent and long-lived (episodic at least during the Noachian and Hesperian) shield volcano that developed in a water-enriched region of Mars (Scott et al., 1993, 1995). *Interpretation:* Magma–water interaction evidence includes parts of the shield volcano that broke away to contribute to the formation of the chaotic terrain, a system of channels that source at the southern margin of a late Hesperian lava flow, channels that dissect plains-forming materials, and a basal scarp similar to the scarp located at the base of Olympus Mons. Valley networks that dissect the upper reaches of the volcano may have formed by both endogenic- and climate-induced activity. Such long-lived magma and water interactions point towards a pronounced hydrothermal environment in the geologic and paleohydrologic records.
2	Elysium rise volcanic province	Hesperian – Amazonian {1,2,3,4,5,7,8}	Shield volcanoes, lava fields, faults, channel systems, and depressions (Greeley and Guest, 1987; Tanaka et al., 2005). *Interpretation:* Magmatic complex that has evolved in a water-enriched region of Mars (e.g., Mouginis-Mark et al., 1984; Mouginis-Mark, 1985), similar in many respects to Tharsis, but smaller, much less complex and long-lived.
3	Nili Fossae	Noachian {1,2,3,4,5,7,8}	Detection of hydrated phyllosilicates by OMEGA visible-infrared spectroscopy and detection of olivine by TES. Thin unaltered mafic units rest directly on phyllosilicate-bearing outcrops (Bibring et al., 2006). *Interpretation*: Complex of grabens and fractures related to the formation of the Isidis impact basin (Hoefen et al., 2003), but basalt floors of Nili Fossae made up from lava by Syrtis Major volcanic complex. Phyllosilicates indicate long-duration exposure to water and weathering in the shallow subsurface due to low grade hydrothermal alteration (Mustard et al., 2006).
4	Hadriaca/Tyrrhena volcanic province	Late Noachian–early Amazonian, and possibly younger activity {1,2,3,4,5,8}	Volcanic province, which includes volcanoes, lava flow fields, systems of wrinkle ridges, flows of diverse origins, and outflow channels (e.g., Greeley and Guest, 1987; Crown et al., 1992). *Interpretation*: Site of magma and water interactions, as well as climate-induced phenomena.
5	Northwestern Slope Valleys (NSVs)/Mangala Valles	Noachian–late Amazonian {1,2,4,5,7,8}	Lava flows, faults, valleys, Mangala Valles outflow channel system, sapping channels, dark slope streaks, elevated chlorine, magnetic and gravity anomalies. *Interpretation:* Prime candidate site for the future exploration based on multiple layers of geologic, topographic, geophysical, and elemental information including the highest concentration of chlorine recorded on the planet (Boynton et al., 2004; Dohm et al., 2006).
6	West Candor Chasma, Valles Marineris	Noachian to late Amazonian {1,2,3,4,6,8}	Candor Chasma is an east-trending trough of the Valles Marineris canyon system comprised of canyons, grabens, pit craters, and channels. Hydrated sulfates have been identified near layered materials interpreted to be volcanic by the Omega instrument on Mars Express (Gendrin et al., 2005). *Interpretation:* The detection of kieserite, gypsum, and epsomite or more complex sulfate molecules (e.g., Gendrin et al., 2005) indicate eolian and/or volcanic deposition of materials into aqueous environments, which is consistent with Viking-based interpretations (e.g., Lucchitta, 1987).
7	Tharsis: Central Valles Marineris rise	Late Noachian–early Hesperian and possibly younger activity {1,2,3,4,7,8}	Topographic rise marked by faults that are radial and concentric about the central part of Tharsis (e.g., Dohm et al., 2001a, 2001b, 2001c), canyons (e.g., Witbeck et al., 1991), valleys in places (e.g., Mangold et al., 2004). *Interpretation*: Plume-driven uplift along a major crustal zone of weakness in the central part of an ancient, Noachian basin/aquifer system (Dohm et al., 2001a), as part of the growth of a tectono-magmatic complex, similar in many respects to those identified on Earth (Komatsu et al., 2004a).
8	Cerberus plains/Marte Vallis	Late Hesperian–Amazonian {1,2,3,4,5?,8}	Lava plains cut by faults, which includes Cerberus Fossae; valley systems such as Athabasca Valles that sources from Cerberus Fossae (Burr et al., 2002), as well as Marte Valles that connects Elysium and Utopia basins (Scott et al., 1995); topographic highs, some of which display summit pits. *Interpretation*: Site of geologically recent magma/tectonic/water activity, evidence of which includes structurally controlled release of water to form Athabasca Valles, floodwaters to incise Marte Valles, as a putative spillway between Elysium and Utopia paleolakes (Scott et al., 1995), and phreatomagmatic explosions due to the emplacement of lava flow materials over a volatile-rich substrate to form rootless cones, among other possibilities (e.g., crater statistics of some of these lava surfaces in this region exhibit model ages of less than 10 Ma; Lanagan et al., 2001). The Cerberus Plains are covered by some of the recent flood lava (Keszthelyi et al., 2000), and the "Cerberus Fossae" were identified as likely vents for some or all of the lava flows. In addition to lava–water interactions (Plescia, 1990, 2003), other investigators pointed out other manifestations including permafrost mounds (pingos) (e.g., Murray et al., 2005; Page and Murray, 2006).

Table 1 (*continued*)

9	Tharsis: Warrego rise	Late Noachian–early Hesperian, and possibly younger activity {1,2,3,4,5?,8}	Highest promontory within the Noachian Thaumasia highlands mountain range that records complex structure and magnetic signatures; well-developed valley networks of Warrego Valles; similar trending pit crater chains and complex rift systems and elongated depressions at the source region of Warrego Valles; impact craters, ridges, fractures, and fault systems of varying trends and erosional/deformational states. *Interpretation*: Concentration of plume-driven magmatic/tectonic activity and associated valley development, which includes possible local precipitation (e.g., Gulick et al., 1997; Dohm and Tanaka, 1999; Anderson et al., 2001; Ansan and Mangold, 2006). Warrego Valles appeared to have formed concurrently with nearby fault and rift systems and collapse pits and depressions, and faults appear deflected about the source region (Scott and Dohm, 1990).
10	Malea Planum volcanic province	Late Noachian–early Hesperian, and possibly younger activity {1,2,3,4,5?,8}	Volcanic province that partly infills an ancient paleovalley, which includes volcanoes, lava flow fields, and valleys (e.g., Greeley and Guest, 1987). *Interpretation*: Site of magma and water interactions (including phreatomagmatic eruptions and hydrothermal alteration) and climate-induced activity, as well as possible glaciation or volatile-driven catastrophic flooding (Tanaka et al., 2002) that may have chiseled the terrain. GRS-data is consistent with such interpretation (Taylor et al., 2006).

to be prevalent in the impact-controlled volcanic provinces as well. Also, seemingly isolated volcanic constructs such as Apollinaris Patera (Scott et al., 1993; Robinson et al., 1993) and promontories in the Chasma Borealis region interpreted to be volcanic (Dial et al., 1994) may have been involved in the interaction of magma and water. In the particular case of the prominent and long-lived (episodic at least during the Noachian and Hesperian) shield volcano, Apollinaris Patera (Target 1 in Table 1; Fig. 2.1), located between the highland–lowland boundary to the north of the major vent structure and Gusev impact crater to the south, evidence for magma and water interactions include parts of the volcano that have broken away to form chaotic terrain and a network of valleys along the southern margin of the Hesperian lava flow that was emplaced on the southern flank of the volcano (Scott et al., 1993). In addition, a prominent scarp that forms the base of the volcano, similar to the basal scarp for Olympus Mons, has been interpreted as a wave-cut platform among other possible hypotheses (e.g., Scott et al., 1993). This kind of geologic history with recorded magma–water interactions is consistent with Gamma Ray Spectrometer-based elemental information that indicates elevated hydrogen and chlorine when compared to the rest of the equatorial region of Mars (Boynton et al., 2004; Dohm et al., 2006; Keller et al., 2006; Taylor et al., 2006). Although the elevated chlorine signature could also be attributed to the complex lithologic nature of the region (Scott and Tanaka, 1986; Scott et al., 1993), other processes such as aeolian deposition of Cl-rich dust, acid-fog reactions associated with volcanic exhalations, and water transport and evaporite deposition are viable explanations for the Cl signature (Keller et al., 2006; Taylor et al., 2006). As such, Cl by itself may not be indicative of aqueous environments let alone hydrothermal activity, but when coupled with other criteria elevate the potential that such environments exist on Mars. A summary of candidate hydrothermal targets deriving from endogenic activity is provided in Tables 1 and 2 (also see corresponding Figs. 1 and 2). Whereas Table 1 and corresponding Fig. 2 provides the top candidate targets based largely on the total number of selection criteria, those listed in Table 2 remain candidate targets though with fewer observable selection criteria.

2.2. *Exogenic, impact-induced activity and associated candidate hydrothermal environments*

Impact craters of varying sizes, degrees of preservation (from pristine to highly degraded), and morphologic characteristics mark an active exogenic-induced history at the martian surface. The presence of significant amounts of ground ice or water would cause impact-induced hydrothermal alteration at martian impact sites and nearby surroundings. Several lines of evidence point to a dramatic increase in the number of impact events at ∼3.9 Ga (Tera et al., 1974; Cohen et al., 2000), which coincides with the earliest isotopic evidence of life on Earth at ∼ 3.85 Ga (Mojzsis and Harrison, 2000) and opens the possibility that life may have been transferred from Earth to Mars or vice versa via impact panspermia (Melosh, 1988). This period, often referred to as the Lunar Cataclysm, lasted 20–200 million years (Abramov and Kring, 2005; Strom et al., 2005), during which time hydrothermal heat generated by impact events may have exceeded that generated by volcanic activity (Kring, 2000).

The primary heat source of a hydrothermal system associated with a complex impact crater is likely shock-emplaced heat. Physical manifestations of impact craters include the central uplift and melt sheet as observed, for example, in Gusev, Gale, and Boeddicker craters (for locations, see Fig. 1). Newsom et al. (1996) showed that the thermal energy of the impact melt and the central uplift can keep a lake from completely freezing under a thick sheet of ice for thousands of years, even under the current martian climatic conditions. The estimated life time of impact-induced hydrothermal systems on early Mars ranges from 67,000 years for a 30 km crater, 380,000 years for a 180 km crater, to nearly 10 Ma for a Hellas-sized basin, depending strongly on the assumed permeability of the subsurface (Abramov and Kring, 2005). Both geological evidence and modeling suggest that the flow of hydrothermal fluids in large craters will be concentrated at the margins of the melt sheets in zones of higher permeability, focused along the crater rims and central uplifts. Hydrothermal modeling conducted by Rathbun and Squyres (2002) indicated that a lake could form in a large complex impact crater from the associ-

Table 2
Additional candidate targets of endogenic-driven hydrothermal activity on Mars based on total number of selection criteria listed in Section 2

#	Name (for location, see Fig. 1)	Relative age and Selection criteria met based on current knowledge	Description/interpretation
11	Chasma Borealis	Amazonian and possibly older activity {1,2,3,5,8}	Prominent valley, polar layered deposits, polygonal-patterned ground, dune fields, and isolated promontories. *Interpretation*: Promontories may be volcanoes (including table top constructs). Valley may be associated with the release of floodwaters related to magma and water interactions or subglacial flow of water (e.g., Dial et al., 1994).
12	West Olympia Undae	Amazonian and possibly older {1,2,4,5,6}	Gypsum, bassanite and aluminum oxide are identified in the western part of Olympia Undae near 245° E, 85° N (Langevin et al., 2005), as well as isolated promontories. *Interpretation*: Some of the promontories have been interpreted to be volcanoes using MOLA (e.g., Garvin et al., 2000) and HRSC data (e.g., Neukum and Gasselt, 2006). The spatial and temporal relations among the putative volcanoes and the identified minerals collectively point to hydrothermal activity as a distinct process in the region.
13	Tharsis: Tempe Terra	Noachian–Amazonian {1,2,3,4,8}	Irregular topography; highly and moderately fractured materials; volcanoes; elongated depressions and pit crater chains, which are aligned with Alba Patera-centered radial fault system; fractures, fault systems, wrinkle ridges, and broad ridges of varying trends and erosional/deformational states; valleys. *Interpretation*: Igneous plateau, which includes a region of long-lived magmatism with tectonic, intrusive, and volcanic activity (e.g., Scott and Dohm, 1990; Dohm et al., 2001a; Moore, 2001).
14	Xanthe Terra	Late Noachian–early Amazonian {1,2,4,5,8}	Undulating, warped, and densely fractured surfaces of highland regions. *Interpretation*: Extensional surface warping related to ground subsidence, caused when pressurized water confined in the subterranean caverns was released to the surface; activity includes water emanations that resulted in the formation of crater lakes and excavation of Ares, Tiu, and Simud Valles of the eastern part of the circum-Chryse outflow channel system. Resurfacing may be linked, in part, to Tharsis: Central Valles Marineris rise, East Valles Marineris, Northeast Valles Marineris, and Kasei (Location 17).
15	Tharsis: East Valles Marineris	Late Hesperian–early Amazonian, but possibly earlier activity {1,2,3,4,8}	Chaotic materials, which include isolated and networking blocks, depressions, and canyons mark a potential source region of outflow channels such as Simud Vallis and Tiu Vallis (Scott and Tanaka, 1986; Witbeck et al., 1991; Rodriguez et al., 2005a, 2005b). *Interpretation*: Magmatic-driven activity, which includes release of floodwaters, collapse, tectonism, similar in many respects to the Tharsis Central Valles Marineris rise with pronounced activity during the late Hesperian and early Amazonian. Possibly linked to activity of Central Valles Marineris rise, as well as other outflow channels sources.
16	Tharsis: Northeast Valles Marineris	Late Hesperian–early Amazonian, but possibly earlier activity {1,2,3,4,5}	Similar to Tharsis: East Valles Marineris, but source region of Maja Valles, which includes promontories. *Interpretation*: Similar to the Tharsis East Valles Marineris, but promontories may mark volcanoes.
17	Tharsis: Kasei	Late Hesperian–early Amazonian, but possibly earlier activity {1,2,3,4,5}	Similar to Tharsis East Valles Marineris, but located near potential source region of Kasei Valles. *Interpretation*: Center of magmatic/tectonic activity (Scott and Dohm, 1990), which may have contributed to the development of Kasei Valles.
18	Tharsis: Alba Patera	Late Hesperian–early Amazonian {1,2,3,4,8}	Construct marked by curvilinear grabens and centrally located depressions; pit crater chains. North flank is dissected by valley networks. *Interpretation*: Concentration of tectonic activity associated with the development of a large shield volcano (Scott and Tanaka, 1986; Anderson et al., 2004); valleys possibly associated with development of shield volcano (e.g., Gulick and Baker, 1990).
19	Tharsis: Aureole deposits of Arsia Mons	Late Hesperian–early Amazonian {1,2,3,4,8}	Aureole deposits, which include 3 facies; faults and depressions that cut Amazonian lava flows (Scott and Zimbelman, 1995). *Interpretation*: Magmatic, tectonic, and geohydrologic activity, as well as climate-induced resurfacing.
20	Tharsis: Aureole deposits of Pavonis Mons	Late Hesperian–early Amazonian {1,2,3,4,8}	Aureole deposits, which include 3 facies; faults and depressions that cut Amazonian lava flows (Scott and Tanaka, 1986). *Interpretation*: Magmatic, tectonic, and geohydrologic activity, as well as climate- induced resurfacing (Scott and Zimbelman, 1995; Shean et al., 2005).
21	Tharsis: Aureole deposits of Ascraeus mons	Late Hesperian–early Amazonian {1,2,3,4,8}	Aureole deposits (Scott and Tanaka, 1986; Scott et al., 1995). *Interpretation*: Magmatic, tectonic, and geohydrologic activity, as well as climate-induced resurfacing (Scott and Tanaka, 1986).
22	Tharsis: Aureole deposits of Olympus Mons	Late Hesperian–early Amazonian {1,2,3,4,8}	Aureole deposits, which include irregular topography, curvilinear ridges, fractures and faults (Morris and Tanaka, 1994). *Interpretation*: Similar to the locales of Arsia Mons, Pavonis Mons, and Ascraeus Mons.

Table 2 (*continued*)

23	Tharsis: Acheron Fossae	Late Hesperian–early Amazonian, and possibly earlier activity {1,2,3,4,8}	Irregular topography, faults, channels (Scott and Tanaka, 1986). *Interpretation*: Magmatic, tectonic, geohydrologic (including mass wasting; e.g., Plescia, 2005) activity, as well as climate-induced resurfacing.
24	Tharsis: West Valles Marineris	Late Noachian–early Hesperian and possibly younger activity {1,2,3,4,8}	Western part of the complex canyon system of Valles Marineris, which includes Noctis Labyrinthus (Scott and Tanaka, 1986; Witbeck et al., 1991). *Interpretation*: Similar to the Central Valles Marineris rise of Tharsis, but concentration of activity pronounced during the late Hesperian, which includes continued growth of Noctis Labyrinthus.
25	Tharsis: Syria Planum	Noachian–late Hesperian, and possibly younger activity {1,2,3,4,8}	Raised north rim; concentric and radial grabens (including Noctis and Claritas Fossae), collapse troughs (Noctis Labyrinthus), and pit crater chains; succession of sheet lavas that bury the feature's southeast rim and infill the feature's interior; small shield volcanoes (Head et al., 2001; Anderson et al., 2004). *Interpretation*: Shield complex and center of long-lived magmatic/tectonic activity (Dohm et al., 2001a, 2001b; Anderson et al., 2001, 2004).
26	Tharsis: Central Thaumasia Highlands	Late Noachian–early Hesperian, and possibly younger activity {1,2,3,4,8}	Rift and fractures and fault systems of varying trends; valley networks dissect the flanks of the promontory and nearby rock outcrops. *Interpretation*: Concentration of tectonic activity associated with the development of the promontory interpreted to be a large volcano (Scott and Tanaka, 1986; Dohm et al., 2001a). Shield volcano development may have accompanied structural uplift along a zone of weakness produced by magmatic/tectonic activity and associated valley development (Tanaka et al., 1998; Dohm and Tanaka, 1999; Dohm et al., 2001b).
27	Tharsis: Southwest Thaumasia Plateau	Late Noachian–early Hesperian, and possibly younger activity {1,2,3,4,8}	Rift and fractures and fault systems of varying trends. Valley networks dissect the southern flank of the promontory and rock outcrops, which occur downslope of the construct along the margin of the Thaumasia Plateau. *Interpretation*: Concentration of tectonic activity associated with the development of the promontory interpreted to be a large volcano (Scott and Tanaka, 1986; Dohm et al., 2001a). Shield volcano development may have accompanied structural uplift along a zone of weakness produced by magmatic/tectonic activity and associated valley development (Dohm and Tanaka, 1999).
28	Meridiani Planum	Noachian and possibly younger {1,5,6,7,8}	Outcrops of sedimentary sequences and mantle-forming materials including sulfate-rich layered deposits with hematite spherules, faults, and valleys. *Interpretation*: Regional heating in the Meridiani Planum is thought to have caused a release of sulfide-rich hydrothermal waters, leading to formation of pyrite-rich regional deposits. Near-surface aqueous oxidation of pyrite formed mineral deposition in acidic solutions, leading to the formation of jarosite assemblages, goethite concretions and, ultimately, coarsed–grained hematite, through an extended diagenetic history. Alternatively, volcanic lapilli have also been suggested as an origin for the hematite concretions (Knauth et al., 2005). Other interpretations include rock materials developed in sabka (Squyres et al., 2004) and hydrothermal (Hynek, 2004) environments.
29	Tharsis NW	Late Hesperian–Amazonian {1,2,4,8}	Modified lava plains, valley system, faults (Mouginis-Mark, 1990). *Interpretation*: Magmatic-driven, structurally-controlled release of water.
30	Ceraunius Tholus	Late Hesperian to Amazonian {1,2,4,8}	Construct with summit depression and channels. *Interpretation*: Volcanic construct and summit caldera dissected by channels, resulting from several mechanisms including snow melt by subsurface heating (Jaumann et al., 2006). The lower flanks of the volcano are buried by plains-forming materials. Valleys cut into the flanks of the volcano and form a delta in the impact crater located just north of Ceraunius Tholus.
31	Tharsis: Southern Coprates	Late Noachian–early Hesperian, and possibly younger activity {1,2,4,8}	Networks of trough-like valley forms, rift and fault systems, depressions, impact craters of varying erosional states, and partly eroded wrinkle ridge materials. The depressions and rift systems are located at the source region of the system of troughs. *Interpretation*: Concentration of magmatic/tectonic activity evident from an apparent process linkage (e.g., spatial and temporal associations) between the troughs, rift systems, and depressions similar in many ways to that proposed for the Galaxias Fossae region, where magmatic-driven activity included the formation of tectonic structures, the migration of volatiles such as ice melt along the fracture and fault systems, and structurally controlled release of water and other volatiles to form channel distributaries (Baker, 1982; Mouginis-Mark, 1985). Also, similar to Warrego rise (Location 9).
32	Tharsis: West Thaumasia Plateau	Late Noachian–early Hesperian {1,2,4,8}	Promontory among faults of Claritas Fossae and irregular depressions; degraded valley networks dissect the flanks of the promontory. *Interpretation*: Concentration of tectonic activity associated with the development of promontory, which is likely to be a large volcano (Scott and Tanaka, 1986; Dohm et al., 2001b) or a relict of an impact event (Craddock and Maxwell, 1993). Shield volcano development may have accompanied structural uplift along a zone of weakness produced by magmatic/tectonic activity or related to a large impact event.

(*continued on next page*)

Table 2 (*continued*)

33	Tharsis: Claritas rise	Noachian {1,3,4,8}	Elongated topographic rise; irregular rugged topography, which includes large promontories comprising highly- and moderately-fractured materials; impact craters, ridges, fractures, fault and rift systems of varying trends and erosional/deformational states; outcrops of dissected materials in places. *Interpretation*: Basement complex and other highly deformed rock materials (possibly including mantled granite/grano-diorite), which is also a prominent magnetic anomaly (Mitchell et al., 2007); primary center of tectonic activity related to magmatic-driven uplift along a zone of weakness and associated tectonic and hydrothermal activity (Dohm et al., 2001a; Anderson et al., 2001).
34	White Rock	Noachian and possibly younger {1,8}	White rock materials within an impact crater. *Interpretation*: Aqueous or aeolian interpretations; White Rock may be a lacustrine sedimentary sequence (Williams and Zimbelman, 1994), precipitation of a lens of magnesium carbonate where ground water seeped into an ancient evaporating lake (Russel et al., 1999), or an eroded accumulation or weakly cemented aeolian sediment (Ruff et al., 2001). Magmatic activity may have also contributed to its occurrence. Possible concurrence of volcanic features and evaporites make it an intriguing target.

ated heat of the impact, even under current martian atmospheric conditions.

Impact craters may have played an important role in aqueous and geochemical processes in the surface/near-surface environment of Mars, including geomorphic expression, chemical transport, and soil formation. Exogenic impact-driven hydrologic activity may include valley formation (e.g., Carr and Head, 2003) within a freezing dry climate (Shuster and Weiss, 2005), and ground-water sapping, runoff, mass wasting, and/or episodic flooding (Pieri, 1976; Baker and Partridge, 1986; Carr, 1995) largely due to hydrothermal circulation (e.g., Newsom, 1980; Brakenridge et al., 1985; Tanaka et al., 1998; Segura et al., 2002). A major amount of ice could be melted by shock heating during the impact event, forming fluvial valleys (Gulick, 1998). Outbursts of groundwater on Mars appear to be associated in time and space with impact-induced fracturing and lateral and perhaps minor upward transport of water due to seismic pumping such as in the case of the 200-km-diameter Lowell impact crater where seismic energy related to the impact event may have pumped groundwater and perhaps fluidized slurry to the surface from beneath the cryosphere to form valleys and a flow deposit (Tanaka et al., 1998). Large impacts could have generated sufficient seismic activity, liquefying poorly consolidated aquifers at depth and pumping water or slurry to the surface through impact fractures (MacKinnon and Tanaka, 1989; Clifford, 1993). Lampland and Voeykov craters, which formed along the southern margin of the Thaumasia plateau (Dohm et al., 2001b; also see Fig. 1 for locations), may exemplify impact-induced valley formation only where favorable hydraulic conditions governed by topography and structure existed (Tanaka et al., 1998).

The formation of large craters on Mars may also have resulted in the mobilization of salts onto the surface of Mars. Recent fieldwork at terrestrial craters and examination of drill core material from the ejecta blankets suggest that the blanket is far more important for geochemical transport and hydrothermal alteration in small craters than had previously been realized (Newsom et al., 2003). In addition, the central uplift in large craters on Mars can provide a substantial source of heat, equivalent to the heat produced by the impact melt sheet (e.g., Thorsos et al., 2001). Therefore, large impact craters on Mars should have contained sufficient residual heat after their formation to power extensive hydrothermal systems. Subsequent erosion or cratering may have excavated the hydrothermal deposits, making them now available for robotic sampling.

Some of the walls and central peaks of impact craters (e.g., Hale crater) are dissected by gullies. Gullies on Mars indicate liquid water in the recent past and even perhaps under current martian conditions (Heldmann et al., 2005; Malin et al., 2006). In some regions, a crater may display gullies while nearby craters are void of gullies. An example is Hale (gullies) and Bond (no gullies; see Fig. 1 for locations) craters, respectively. The gullied regions in Hale crater show low nighttime temperatures (interpreted to be caused by unconsolidated material), while higher temperature slope-forming materials (interpreted to be consolidated material) occur in the Bond crater (Reiss et al., 2004). These observations and interpretations are consistent with the morphology observed using Mars Orbiter Camera (MOC) images (Reiss and Jaumann, 2002).

The best-studied impact crater is probably Gusev crater. The crater appears to be an old crater-lake bed, filled with rock materials up to 1 km thick. Some exposed outcrops also indicate faint layering. The channel system, Ma'adim Vallis, drains into Gusev crater (Cabrol et al., 1998; Kuzmin et al., 2004), possibly contributing to the formation of a lake (Cabrol and Grin, 2001), though evidence may be obscured by impact cratering and wind-related activity, among other processes (Cabrol et al., 2006). Spirit, one of NASA's two Mars Exploration Rovers (MER), landed in Gusev crater and has been collecting new information, which includes possible hydrothermal alteration and transport of mobile elements (Gellert et al., 2004). Gusev crater certainly meets selection criteria 1, 6, and 8, but we deem the available information for most craters (including Gusev) to uncertain to assign selection criteria at the present time. Furthermore, impact craters are notoriously covered up by other sediments or have been significantly altered by geological processes.

3. Terrestrial analog environments of endogenic-induced hydrothermal activity

Hydrothermal activity is present within Earth's crust wherever heat and water coexist, involving heated aqueous solutions created under a range of conditions including geysers, fumaroles, and hot springs. Heat sources may be diverse and derive from any type of igneous activity, large-scale tectonism, or the geothermal gradient (Gardner et al., 1995), all of which may be associated with endogenic activity. Hydrothermal activity could also be induced by impact cratering events if any phase of water exists in the subsurface (e.g., Abramov and Kring, 2005).

Given the abundant and diverse records of hydrothermal activity on Earth that appear to have similar identifiers to those of candidate targets on Mars described above, terrestrial hydrothermal environments (ancient and extant) form the proving grounds for developing the means to optimally identify, map, home in on, and sample these environments. For example, the deposits of gray hematite found at Sinus Meridiani on Mars are also identified in geologic terrains on Earth where there has been standing water, particularly in hot springs enriched in minerals. Examples include: (1) the Yellowstone region (Hellman and Ramsey, 2004); (2) the Tinto River region that sources in the Iberian Pyritic Belt and produces one of the largest hydrothermally-induced deposits of metallic sulfides in the world (e.g., Boulter, 1996; Leistel et al., 1998); and (3) the Colorado Plateau where 'blueberries' are interpreted to be the result of variable redox conditions in underground fluids (Chan et al., 2004). Extensive surficial deposits, however, can also form in environments with modern endogenic-derived cold springs (Crossey et al., 2006). The Yellowstone Caldera is the world's largest hydrothermal system that is fed by a hot spot located beneath the continental crust. From the numerous and widespread ancient and extant hydrothermal environments on Earth that could be considered as potential martian analogs, we describe Valles Caldera and the White Sands regions in detail below, as they both record endogenic-driven hydrothermal activity, acidic aqueous conditions, and brines consistent with recent findings based on the Mars Global Surveyor (MGS), MER, and Mars Express missions (Hynek et al., 2002; Rieder et al., 2004; Gendrin et al., 2005).

3.1. Valles Caldera region

The geologic setting of the Valles Caldera region includes volcanic rocks, which overlie Precambrian granite, gneiss, and schist, as well as sedimentary rocks including evaporites of the Colorado Plateau. The basement rocks are faulted and progressively dip eastward toward the Rio Grande rift, where Tertiary sediments of different stages of induration overlie the fault blocks. The caldera formed during the Quaternary eruption of the Bandelier Tuff, producing a series of concentric fractures and faults; the caldera's interior is filled with rhyolite domes, lava flows, and tuffs (Doell et al., 1968; Goff and Grigsby, 1982). The caldera is located at the intersection of regional lineaments where carbonate-rich water, high in total dissolved solids, is percolating up through the fracture zones at various locations (e.g., Jemez Springs, Soda Dam Spring), similar to the hydrogeologic activity described for Mars (e.g., Dohm et al., 1998a, 1998b; Tanaka et al., 1998).

The Valles Caldera region hosts high-temperature ($\leqslant 300\,^{\circ}C$) hydrothermal systems with several geothermal springs that discharge waters of different chemical composition (Goff and Gardner, 1994; Truesdell and Janik, 1986; Sass and Morgan, 1988). Water samples of the Sulfur Springs area, for example, have shown acidity with pH values ranging from 1.40 to 1.98 and very high concentrations of sulfate ions (Rzonca and Schulze-Makuch, 2003). These kinds of fluids originate from the condensation of steam and the oxidation of H_2S forming natural sulfuric acid (Goff and Gardner, 1994). There are hydrothermal waters of other chemical compositions at the Valles Caldera as well as carbonate-rich waters. Bacterial analyses revealed large contents of biomass in the Sulfur Springs samples, significantly higher than in any other springs of the Valles Caldera (Rzonca and Schulze-Makuch, 2003), indicating that acidic environments such as the Sulfur Springs area provide suitable microbial habitats.

The Valles Caldera region displays many of the identifiers reported for the candidate hydrothermal targets of Mars provided in Tables 1 and 2. Analogous putative hydrothermal locales on Mars are central Valles Marineris and the Warrego rise (Locations 7 and 9 in Table 1, respectively). Detailed mapping shows faults radial and concentric about central Valles Marineris, interpreted to be the result of plume-driven tectonism and associated uplift, dike intrusion, volcanism, and hydrothermal activity (Dohm et al., 1998a, 1998b; 2001a, 2001b, 2001c; Anderson et al., 2001). The Valles Caldera is related to a rift process that at present time appears to be inactive (Rio Grande Rift). Water migrates upwards through deep fracture zones at regional scale and locally heated from a magma chamber below. This mechanism has been proposed for several of the putative magmatic-driven locations on Mars shown in Tables 1 and 2.

3.2. White Sands region

The White Sands analog site in southern New Mexico is of special relevance, because of the recent discovery of hydrothermal fluids that discharge into a sulfate-rich playa. White Sands National Monument is best known as the largest field of gypsum dunes in the world (McKee, 1966; McKee and Moiola, 1975; Schenk and Fryberger, 1988). Lake Lucero, a highly saline playa within White Sands National Monument, is covered by water about 10% of the year. The playa with its associated dune fields is very diverse in its composition, texture, and ecosystem. Lake Lucero, situated in the Tularosa basin of southern New Mexico, is a Holocene feature, and its hydrothermally emplaced sediments are incised into older Pleistocene lacustrine sediments of Lake Otero. During its final phase, thick beds of coarse-grained gypsum were deposited along with the lacustrine clay, beach sands, and deltaic sediments. The White Sands area is underlain by intrusive and extrusive rocks associated with the Rio Grande Rift. The Rio Grande rift formed by extensional tectonism, which occurred during the last 35 Ma. (Chapin and Cather, 1994). There are several major faults within the rift zone, which penetrate deep within the Earth's crust (Mailloux et al., 1999), acting as conduits for the percolation of deep hydrothermal fluids and gases to the surface (Newell et al., 2005). Recent investigations showed the discharge of previously unknown hydrothermal water to the Lake Lucero area, a discovery supported by (1) the detection of the microbe *Methanosaeta thermoacetophila* in water obtained from a piezometer screened into Lake Lucero, (2) the presence of hydrothermal minerals in the soil, (3) elevated ground-water temperatures, and (4) a high ^{18}O isotope fractionation inconsistent with salinity effects alone (Schulze-Makuch, 2002). Not only does the White Sands region provide the eolian, evaporite-rich desert setting similar to past and present environments on Mars, but also the acidic aqueous conditions hypothesized (Fairén et al., 2004) and later corroborated for Mars through MER-based investigations (Catling, 2004). White Sands has been compared to White Rock on Mars in the past, which has been interpreted as an eroded remnant of a lacustrine deposit (Williams and Zimbelman, 1994). However, recent spectra of the White Rock area indicating the lack of hydrates, sulfates, carbonates, and hydroxides at White Rock raise doubts about that analogy.

4. Terrestrial analog environments of exogenic-induced hydrothermal activity

Hydrothermal activity on Earth induced by impacts has been well studied. These exogenic-induced environments are potential martian analogs (e.g., Farrow and Watkinson, 1992; Naumov, 2002; Ames et al., 1998, 2004; Hecht et al., 2004; Zurcher and Kring, 2004). The post-impact hydrothermal activity is well documented at terrestrial craters with alteration mineral assemblages from various impact craters (e.g., McCarville and Crossey, 1996; Naumov, 2002), though no active impact-induced hydrothermal site has been reported to date. Kring (2000) pointed out several impact craters that show evidence of hydrothermally altered secondary minerals and saline fluid inclusions in minerals. Examples are the Chicxulub, Manson, Puchezh–Katunki, Saint Martin, Siljan, and Sudbury impact craters. Large hydrothermal systems were created in and around the central uplifts of complex craters reaching in some cases the crater rim (e.g., Siljan). The hydrothermal system of Puchezh–Katunki extended to a depth of at least 5 km in the uplifted peak (Pevzner et al., 1992). The impact crater has a diameter of about 40 km and the melt sheet is about 65 m thick about 11 km from the center of the crater (Simonds and McGee, 1979). Even in small craters such as Lonar crater (1.8 km in diameter), substantial hydrothermal alteration has occurred, probably due to the thermal effects of the impact event (Hagerty and Newsom, 2003).

An especially suited analog crater on Earth is Haughton crater. The polar desert environment is comparable to prevailing martian environmental conditions, which includes cold, dry, windy, rocky, dusty, and almost unvegetated conditions with elevated ultraviolet light (Lee, 2002). The impact crater, which has a diameter of about 20 km, is studied by investigators of the NASA Haughton-Mars Project. The team of investigators discovered remnant signatures of ancient hydrothermal activity such as hot springs and lakes, as well as post-impact hydrothermal deposits along the crater rim (Osinski et al. 2001, 2005). These hot spring features originated from the transmittal of impact-induced heat into the surrounding rocks. Networks of channels located outside of Haughton crater bear similarities to the small martian valley networks (Lee, 2002), implying that the valley networks around the martian craters may also be related to both impact-induced activity and subsequent water/mudflows.

5. Exploration strategies

The notion of Mars as a water-enriched, still possibly internally active planet is supported by the recent acquisition of geologic, hydrologic, topographic, chemical, and elemental information obtained by the Mars Global Surveyor (MGS), Mars Odyssey, Mars Express, and Mars Exploration Rovers (MER). The availability of water throughout martian history and its possible existence up to the present time, as well as the dynamic interactions among water and endogenic and exogenic events, render Mars a prime target for astrobiological investigations. Once life would have gained a foothold on Mars, it would be expected to adapt to the changing conditions on the planet (e.g., Schulze-Makuch et al., 2005a; Fairén et al., 2005; Houtkooper and Schulze-Makuch, 2007). In this case, we could expect to find life in microscopic form in subterranean environments such as in ground-water or in caves, and most likely in environments that are currently hydrothermally active (if they exist). Given this potential, how can we best home in on such prime candidate targets of elevated life-containing potential?

An ever-expanding list of candidate hydrothermal targets should be compiled for which this paper would lay the foundation. Both fossil and extant hydrothermal environments should be listed based on rigorous selection criteria incorporating the latest results from Mars missions. Prime targets could be selected now by evaluating the candidate targets described here using existing and yet-to-be-released remote stratigraphic, geomorphic, topographic, spectral, geophysical, and elemental information provided by the instruments onboard the Mars orbiters and the Sojourner and Mars Exploration rovers. The Mars Reconnaissance Orbiter (MRO) has just been inserted into orbit as of this writing. The MRO instrument suite includes the High Resolution Imaging Science Experiment (HIRISE) with a pixel resolution of 30–60 cm and the Compact Reconnaissance Imaging Spectrometer for Mars (CRISM) with a visible/near infrared hyperspectral capability to spatial resolutions of 18 m. Both may provide geological context for the proposed hydrothermal locations, including the possible identification of local zones of hydrothermal-related mineralization through the CRISM instrument. CRISM will improve the quality of near-infrared spectral data sets currently collected by the OMEGA instrument on Mars Express, which are useful to understanding the extent of engodenic activity–water interactions. The Shallow Subsurface Radar (SHARAD) will probe the subsurface using radar waves using a 15–25 MHz frequency band in order to get the desired high depth resolution (compared to 1.3 to 5.5 MHz range of MARSIS). The radar wave return, which is captured by the SHARAD antenna, is sensitive to changes in the electrical reflection characteristics of the coarse- and fine-grain materials such as rock and sand, respectively, and any water present in the surface and subsurface. Similar to high-density rock, water is an excellent conductor, and thus will have a strong radar return. Changes in the reflection characteristics of the subsurface, such as layered deposits, should also be visible.

Further capabilities that should be highlighted include Mars Orbiting Laser Altimeter (MOLA) topography, geophysical information such as MGS-based gravity and magnetic data, spectral data including the Neutron Spectrometer, and subsurface sounding radar (Mars Advanced Radar For Subsurface and Ionosphere Sounding) provided by Mars Express. Mars Orbiter Camera (MOC) imagery is available to supplement existing geologic information. MOC imagery may provide significant clues concerning the geologic histories of the locations of special interest. The application of gravity, magnetic, and thermal information (including those data sets that recently have been acquired by MGS) together with MOLA data may help identify intrusive centers and areas of crustal extension not readily visible at the martian surface. Although the spatial resolution is on the order of 500 km, the Gamma Ray Spectrometer (GRS) on Odyssey is a great asset because it is suited to detect elements such as hydrogen, chlorine, calcium, iron, and magnesium, all of which can be used to examine whether hydrothermal activity may have occurred at the candidate target of sufficient spatial extent such as the Northwestern Slope Valleys location and surrounding region (Location 5 in Table 1), and it is capable of sampling both dust and the underlying rock materials up to $\sim 1/3$ m depth (e.g., Boynton et al., 2004). Thermal Emission Spectrometer (TES) data also have a large pixel size (3 km by 6 km) and thus may not capture distinct signatures from small hydrothermal environments, but some environments (such as the Meridiani hematite region mapped by TES; Lane et al., 1999), may be large enough in their spatial extent for TES-based identification.

A comparison of candidate hydrothermal targets on Mars and well-investigated hydrothermal environments on Earth is an obvious exercise. Many environments on Earth exist that have similar identifiers and probably also similar dynamics, history, chemistry, and possibly biological implications. For example, an exhaustive database was established for both the Valles Caldera and White Sands, including chemical data and physical data (Schulze-Makuch, unpublished data). A thorough biological characterization was also completed included Denaturing Gradient Gel Electrophoresis (DGGE) and Phospholipid Fatty Acid (PLFA) analyses (Rzonca and Schulze-Makuch, 2003). Large databases on the Haughton crater and other confirmed impact structures are currently being established such as the "Earth Impact Database," created and managed by the Planetary and Space Science Centre at the University of New Brunswick, Canada.

The above suggested exploration strategy will only yield limited access in the absence of missions that are capable of investigating identified candidate hydrothermal targets. New mission strategies are needed to explore these sites, which may be located in difficult and hazardous terrain such as canyons, caves, mountain regions with rocky terrain and steep slopes, inside craters, and may only produce signatures that are either too faint for remote sensing (via orbiters), or too wide-spread to be explored by single rovers or landers. One of the new promising mission strategies, recently devised by Fink et al. (2005a), appears to be ideally suited for the exploration of hydrothermal target locales. They propose a "tier-scalable reconnaissance" mission concept, which integrates multi-tier (orbit ⇔ atmosphere ⇔ surface/subsurface) and multi-agent (orbiter ⇔ aerial platforms ⇔ rovers, landers, drill rigs, sensor grids) hierarchical mission architectures, not only introducing mission redundancy and safety, but enabling and optimizing intelligent, less constrained, and distributed science-driven exploration of prime locations on Mars and elsewhere, allowing for increased science return, and paving the way towards fully autonomous robotic reconnaissance missions (Fig. 3). A multi-tier, multi-agent hierarchical mission architecture would overcome the inherent challenge of geologic planetary surface exploration: airborne agents (orbiters and blimps/airships) possess overhead perspectives at different length scales/resolutions, which allow for global to local reconnaissance and could provide guidance to ground-based agents (e.g., mobile rover units) for in situ exploration and sampling.

Tier-scalable mission architectures are necessary to optimally perform reconnaissance of hard-to-get-to locales of special scientific interest such as Melas Chasma, the central part of Valles Marineris. For such a location the following deployment and reconnaissance sequence is envisioned [see Fink et al. (2005a, 2006), or Schulze-Makuch et al. (2005b) for further details]: Orbiter(s) scout areas of scientific interest at a global to regional scale and subsequently insert airborne agents such as balloons, blimps, or airships, which deploy in mid-air above the canyon system for further scouting and testing of hypothesized conditions. If one (or more) of the airborne agents were to detect scientifically interesting features, such as a volatile release (methane plume or water vapor) or elevated heat flow, this airborne agent(s) would then map out, for example, methane concentration profiles and acquire terrain images of the locales of extant hydrothermal activity. The information so obtained from the airborne vantage would subsequently be processed through automated feature-extraction algorithms (e.g., Fink et al., 2005b) and analyzed by science prioritization algorithms while en route (e.g., Fink, 2006; Fink et al., 2005b; Furfaro et al., 2006) to choose prime targets for in situ investigation and sampling by subsequently deployed ground-based agents (small rovers, networks of sensors, etc.). At the respective targets, the rovers would conduct in situ science experiments and thereby gather data that complement the remote sensing data obtained by the airborne agents (e.g., blimps and orbiters).

6. Conclusions

We presented a list of candidate locations for endogenic- and exogenic-driven hydrothermal environments on Mars based on a set of selection criteria as a first step to narrow down potential hydrothermal targets for future exploration. We encourage further evaluation of candidate targets (including those not included in the preliminary list) using existing and yet-to-be-released remote information provided by the instruments on-

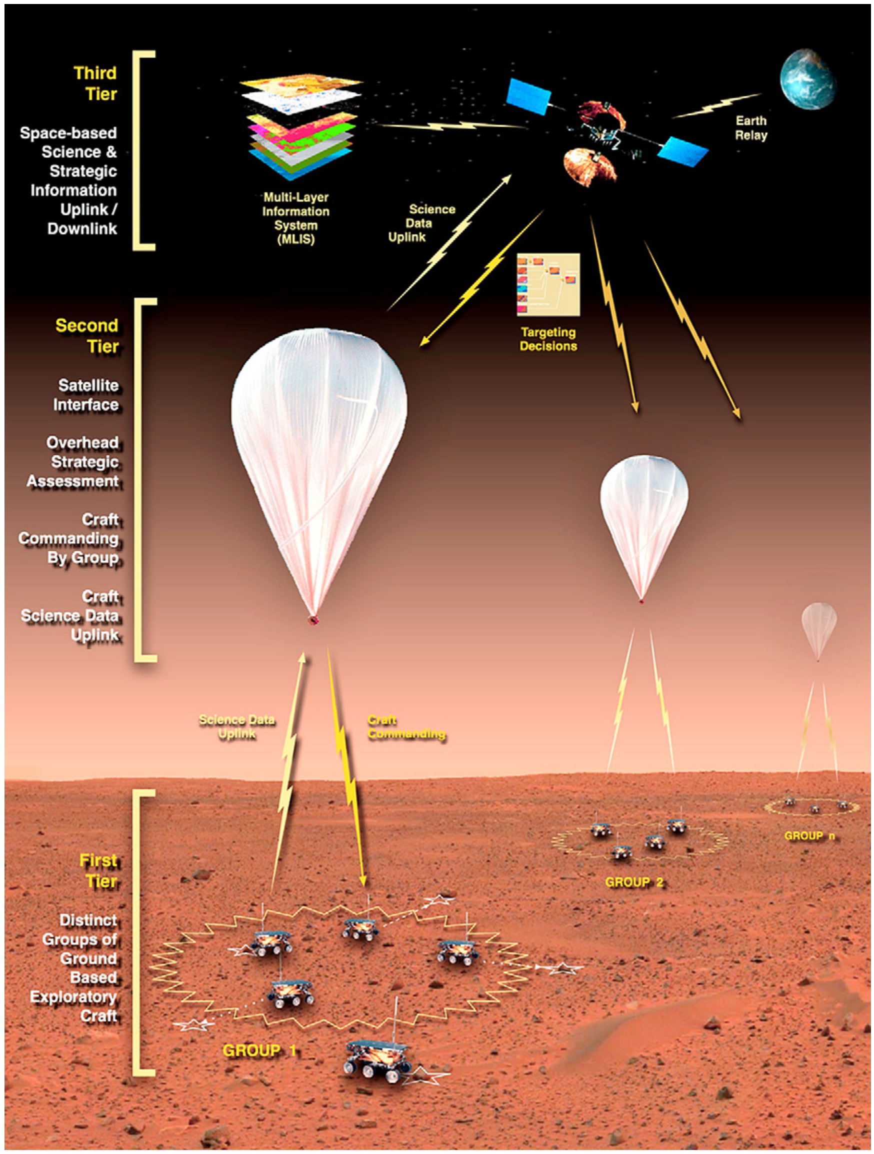

Fig. 3. Tri-level hierarchical multi-agent architecture for autonomous remote planetary exploration of Mars (from Fink et al., 2005a).

board the Mars orbiters and rovers, and suggest future missions based on a novel integrated multi-tier, multi-agent reconnaissance mission concept.

Acknowledgments

We express our sincere thanks to Trent Hare who provided the 3-dimensional topographic images for Fig. 2 to us. We also thank William Boynton, Kris Kerry, and the rest of the Gamma Ray Spectrometer Science Team members, as well as Robert C. Anderson, Justin C. Ferris, and Kenneth L. Tanaka, for their input. We appreciate the constructive comments we received from Laura Crossey and an anonymous reviewer.

References

Abramov, O., Kring, D.A., 2005. Impact-induced hydrothermal activity on early Mars. J. Geophys. Res. 110. E12S09.
Ames, D.E., Watkinson, D.H., Parrish, R.R., 1998. Dating of a regional hydrothermal system induced by the 1850 Ma Sudbury impact event. Geology 26, 447–450.
Ames, D.E., Kjarsgaard, I.M., Pope, K.O., Dressler, B., Pilkington, M., 2004. Secondary alteration of the impactite and mineralization in the basal tertiary sequence, Yaxcopoil-1, Chicxulub impact crater, Mexico. Meteor. Planet. Sci. 39, 1145–1167.
Anderson, R.C., Dohm, J.M., Golombek, M.P., Haldemann, A., Franklin, B.J., Tanaka, K.L., Lias, J., Peer, B., 2001. Significant centers of tectonic activity through time for the western hemisphere of Mars. J. Geophys. Res. 106, 20563–20585.
Anderson, R.C., Dohm, J.M., Haldemann, A.F.C., Hare, T.M., Baker, V.R., 2004. Tectonic histories between Alba Patera and Syria Planum, Mars. Icarus 171, 31–38.
Ansan, V., Mangold, N., 2006. New observations of Warrego Valles, Mars: Evidence for precipitation and surface runoff, Planet. Space Sci. 54, 219–242.
Baker, V.R., 1982. The Channels of Mars. Univ. of Texas Press, Austin.
Baker, V.R., Partridge, J.B., 1986. Small martian valleys: Pristine and degraded morphology. J. Geophys. Res. 91, 3561–3572.
Baker, V.R., Strom, R.G., Gulick, V.C., Kargel, J.S., Komatsu, G., Kale, V.S., 1991. Ancient oceans, ice sheets and the hydrological cycle on Mars. Nature 352, 589–594.

Bibring, J.-P., and 52 colleagues, 2006. Global mineralogical and aqueous Mars history derived from OMEGA/Mars Express data. Science 312, 400–404.

Boulter, C.A., 1996. Did both extensional tectonics and magmas act as major drivers of convection cells during the formation of the Iberian Pyritic Belt massive sulfide deposits? J. Geol. Soc. London 153, 181–184.

Boynton, W.V., and 24 colleagues, 2002. Distribution of hydrogen in the near surface of Mars: Evidence for subsurface ice deposits. Science 297, 81–85.

Boynton, W.V., and 28 colleagues, 2004. The Mars odyssey gamma-ray spectrometer instrument suite. Space Sci. Rev. 110, 37–83.

Brakenridge, G.R., Newsome, H.E., Baker, V.R., 1985. Ancient hot springs on Mars: Origins and paleoenvironmental significance of small martian valleys. Geology 13, 859–862.

Burr, D.M., McEwen, A.S., Sakimoto, S.E.H., 2002. Recent aqueous floods from the Cerberus Fossae, Mars. Geophys. Res. Lett. 29, doi:10.1029/200GL013345.

Cabrol, N.A., Grin, E.A., Landheim, R., Kuzmin, R.O., Greeley, R., 1998. Duration of the Ma'adim Vallis/Gusev crater hydrogeologic system, Mars. Icarus 133, 98–108.

Cabrol, N.A., Grin, E.A., 2001. The evolution of lacustrine environments on Mars: Is Mars only hydrologically dormant? Icarus 149, 291–328.

Cabrol, N.A., Farmer, J.D., Grin, E.A., Richter, L., Soderblom, L., Li, R., Herkenhoff, K., Landis, G.A., Arvidson, R.E., 2006. Aqueous processes at Gusev crater inferred from physical properties of rocks and soils along the Spirit traverse. J. Geophys. Res. 111. E02S20.

Carr, M.H., 1979. Formation of martian flood features by release of water from confined Aquifer. J. Geophys. Res. 84, 2995–3007.

Carr, M.H., 1995. The martian drainage system and the origin of valley networks and fretted channels. J. Geophys. Res. 100, 7479–7507.

Carr, M.H., Head, J.W., 2003. Oceans on Mars: An assessment of the observational evidence and possible fate. J. Geophys. Res. 108 (E5). 5042.

Catling, D.C., 2004. On Earth, as it is on Mars? Nature 429, 707–708.

Chan, M.A., Beitler, B., Parry, W.T., Ormo, J., Komatsu, G., 2004. A possible terrestrial analogue for haematite on Mars. Nature 429, 732–734.

Chapman, M.G., Tanaka, K.L., 2001. Interior deposits on Mars: Subice volcanoes? J. Geophys. Res. 106, 10087–10100.

Chapin, C.E., Cather, S.M., 1994. Tectonic setting of the axial basins of the northern and central Rio Grande rift. In: Keller G.R., Cather S.M. (Eds.), Basins of the Rio Grande Rift: Structure, Stratigraphy, and Tectonic Setting. Geological Society of America Special Paper 291, pp. 5–25.

Christensen, P.R., and 25 colleagues, 2001. The Mars Global Surveyor Thermal Emission Spectrometer experiment: Investigation description and surface science results. J. Geophys. Res. 106, 23823–23871.

Clifford, S.M., 1993. A model for the hydrologic and climatic behavior of water on Mars. J. Geophys. Res. 98, 10973–11016.

Clifford, S.M., Parker, T.J., 2001. The evolution of the martian hydrosphere: Implications for the fate of a primordial ocean and the current state of the northern plains. Icarus 154, 40–79.

Cohen, B.A., Swindle, T.D., Kring, D.A., 2000. Support for the lunar cataclysm hypothesis from lunar meteorite impact melt ages. Science 290, 1754–1756.

Craddock, R.A., Maxwell, T.A., 1993. Geomorphic evolution of the martian highlands through ancient fluvial processes. J. Geophys. Res. 98, 3453–3468.

Crossey, L.J., Fischer, T.P., Patchett, P.J., Karlstrom, K.E., Hilton, D.R., Huntoon, P., Reynolds, A.C., 2006. Dissected hydrologic system at Grand Canyon: Interaction between upper world and lower world waters in modern springs and travertine. Geology 34, 25–28.

Crown, D.A., Greeley, R., 1993. Volcanic geology of Hardriaca Patera and the eastern Hellas region of Mars. J. Geophys. Res. 98, 3431–3451.

Crown, D.A., Price, K.H., Greeley, R., 1992. Geologic evolution of the east rim of the Hellas basin, Mars. Icarus 100, 1–25.

Dial, A.L., Scott, D.H., Dohm, J.M., 1994. Geologic map of science study area 4, Chasma Boreale region of Mars: US Geological Survey Miscellaneous Investigations Series Map I-2357 (1:500,000 scale).

Doell, R.R., Dalrymple, G.B., Smith, R.L., Bailey, R.A., 1968. Paleomagnetism, potassium–argon ages, and geology of rhyolites and associated rocks of the Valles Caldera, New Mexico. Mem. Geol. Soc. Am. 116, 211–248.

Dohm, J.M., Tanaka, K.L., 1999. Geology of the Thaumasia region, Mars: Plateau development, valley, and magmatic evolution. Planet. Space Sci. 47, 411–431.

Dohm, J.M., Tanaka, K.L., Lias, J.H., Hare, T.M., 1998a. Warrego Valles and other candidate sites of local hydrothermal activity within the Thaumasia region, Mars. Lunar Planet. Sci. XXIX.

Dohm, J.M., Anderson, R.C., Tanaka, K.L., 1998b. Digital structural mapping of Mars. Astron. Geophys. 39 (3), 3.20–3.22.

Dohm, J.M., Baker, V.R., Anderson, R.C., Scott, D.H., Rice Jr., J.W., Hare, T.M., 2000. Identifying martian hydrothermal sites: Geological investigation utilizing multiple datasets. Lunar Planet. Sci. XXXI. Abstract 1613.

Dohm, J.M., Ferris, J.C., Baker, V.R., Anderson, R.C., Hare, T.M., Strom, R.G., Barlow, N.G., Tanaka, K.L., Klemaszewski, J.E., Scott, D.H., 2001a. Ancient drainage basin of the Tharsis region, Mars: Potential source for outflow channel systems and putative oceans or paleolakes. J. Geophys. Res. 106, 32942–32958.

Dohm, J.M., Tanaka, K.L., Hare, T.M., 2001b. Geologic map of the Thaumasia region of Mars. US Geol. Survey Map I-2650.

Dohm, J.M., Anderson, R.C., Baker, V.R., Ferris, J.C., Rudd, L.P., Hare, T.M., Rice Jr., J.W., Casavant, R.R., Strom, R.G., Zimbelman, J.R., Scott, D.H., 2001c. Latent activity for western Tharsis, Mars: Significant flood record exposed. J. Geophys. Res. 106, 12300–12314.

Dohm, J.M., Maruyama, S., Baker, V.R., Anderson, R.C., Ferris, J.C., Hare, T.M., 2002a. Evolution and traits of Tharsis superplume. In: Mars, Superplume International Workshop, Abstracts with Programs, Tokyo, pp. 406–410.

Dohm, J.M., Ferris, J.C., Barlow, N.G., Baker, V.R., Mahaney, W.C., Anderson, R.C., Hare, T.M., 2004. The Northwestern Slope Valleys (NSVs) region, Mars: A prime candidate site for the future exploration of Mars. Planet. Space Sci. 52, 189–198.

Dohm, J.M., and 20 colleagues, 2006. Tharsis/Elysium corridor: A marker for an internally active Mars? Lunar Planet. Sci. XXXVII. Abstract 1531.

Fairén, A.G., Dohm, J.M., Baker, V.R., de Pablo, M.A., Ruiz, J., Ferris, J.C., Anderson, R.C., 2003. Episodic flood inundations of the northern plains of Mars. Icarus 165, 53–67.

Fairén, A.G., Fernández-Remolar, D., Dohm, J.M., Baker, V.R., Amils, R., 2004. Inhibition of carbonate synthesis in acidic oceans on early Mars. Nature 431, 423–426.

Fairén, A.G., Dohm, J.M., Uceda, E.R., Rodríguez, A.P., Baker, V.R., Fernández-Remolar, D., Schulze-Makuch, D., Amils, R., 2005. Prime candidate sites for astrobiological exploration through the hydrogeological history of Mars. Planet. Space Sci. 53, 1355–1375.

Farrow, C.E.G., Watkinson, D.H., 1992. Alteration and the role of fluids in NI, Cu and platinum-group element deposition, Sudbury Igneous Complex contact, Onaping Levack area, Ontario. Mineral. Petrol. 46, 611–619.

Feldman, W.C., and 12 colleagues, 2002. Global distribution of neutrons from Mars: Results from Mars Odyssey. Science 297, 75–78.

Fink, W., 2006. Generic prioritization framework for target selection and instrument usage for reconnaissance mission autonomy. In: Proceedings of IEEE World Congress on Computational Intelligence (WCCI) 2006, Vancouver, Canada, pp. 11116–11119.

Fink, W., Dohm, J.M., Tarbell, M.A., Hare, T.M., Baker, V.R., 2005a. Next-generation robotic planetary reconnaissance missions: A paradigm shift. Planet. Space Sci. 53, 1419–1426.

Fink, W., Datta, A., Baker, V., 2005b. AGFA: (Airborne) Automated Geologic Field Analyzer, Symposium SS-56: "New results from the robotic exploration of Mars and Titan and their implications on planetary environmental conditions and cosmochemistry." In: Abstracts of the 15th Annual V.M. Goldschmidt Conference, Moscow, Idaho. Geochim. Cosmochim. Acta 69. 10S, A535.

Fink, W., and 11 colleagues, 2006. Autonomous Tier-Scalable Reconnaissance Missions for remote planetary exploration. In: Proceedings of the 4th International Planetary Probe Workshop 2006, Pasadena.

Furfaro, R., Dohm, J.M., Fink, W., Schulze-Makuch, D., Fairén, A.G., Tarbell, M.A., Hare, T.M., Baker, V.R., 2006. Multi-layer fuzzy logic-based expert system for conducting tier scalable planetary reconnaissance. Lunar Planet. Sci. XXXVII. Abstract 1257.

Gardner, C.A., Scott, K.M., Miller, C.D., Myers, B., Hildreth, W., Pringle, P.T., 1995. Potential volcanic hazards from future activity of Mount Baker, Washington. USGS Open-File Report 95-498.

Garvin, B., Sakimoto, S.E.H., Frawley, J.J., Schnetzler, C.C., Wright, H.M., 2000. Topographic evidence for geologically recent near-polar volcanism on Mars. Icarus 145, 648–652.

Gendrin, A., Mangold, N., Bibring, J.P., Langevin, Y., Gondet, B., Poulet, F., Bonello, G., Quantin, C., Mustard, J., Arvidson, R., LeMouelic, S., 2005. Sulfates in martian layered terrains: The OMEGA/Mars Express view. Science 307, doi:10.1126/science.1109087.

Gellert, R., and 14 colleagues, 2004. Chemistry of rocks and soils in Gusev crater from the alpha particle X-ray spectrometer. Science 305, 829–832.

Gendrin, A., Mangold, N., Bibring, J.-P., Langevin, Y., Gondet, B., Poulet, F., Bonello, G., Quantin, C., Mustard, J., Arvidson, R., LeMouélic, S., 2005. Sulfates in martian layered terrains: The OMEGA/Mars Express view. Science 307, 1587–1591.

Goff, F., Grigsby, C.O., 1982. Valles Caldera geothermal systems, New Mexico, USA. J. Hydrol. 56, 119–136.

Goff, F., Gardner, J.N., 1994. Evolution of a mineralized geothermal system, Valles Caldera, New Mexico. Econ. Geol. 89, 1803–1832.

Greeley, R., Guest, J.E., 1987. Geologic map of the eastern equatorial region of Mars. USGS Misc. Inv. Ser. Map I-1802B (1:15,000,000).

Greeley, R., Thomas, P.E., 1994. Mars landing site catalog. NASA Ref. Pub. 1238, 392 pp.

Gulick V.C., 1993. Magmatic intrusions and hydrothermal systems: Implications for the formation of small martian valleys. Ph.D. thesis, Univ. of Arizona, Tucson, AZ.

Gulick, V.C., 1998. Magmatic intrusions and a hydrothermal origin for fluvial valleys on Mars. J. Geophys. Res. 103, 19365–19387.

Gulick, V.C., Baker, V.R., 1990. Origin and evolution of valleys on martian volcanoes. J. Geophys. Res. 95, 14325–14344.

Gulick, C., Tyler, D., McKay, C., Haberle, R.M., 1997. Episodic ocean-induced CO_2 greenhouse on Mars: Implications for fluvial valley formation. Icarus 130, 68–86.

Hagerty, J.J., Newsom, H.E., 2003. Hydrothermal alteration at the Lonar Lake impact structure, India: Implications for impact cratering on Mars. Meteor. Planet. Sci. 48, 327–478.

Head, J.W., Greeley, R., Golombek, M.P., Hartmann, W.K., Hauber, E., Jaumann, R., Masson, P., Neukum, G., Nyquist, L.E., Carr, M.H., 2001. Geological processes and evolution. Space Sci. Rev. 96, 263–292.

Hecht, L., Wittmann, A., Schmitt, R.T., Stoffler, D., 2004. Composition of impact melt particles and the effects of post-impact alteration in suevitic rocks at the Yaxcopoil-1 drill core, Chicxulub crater, Mexico. Meteor. Planet. Sci. 39, 1169–1186.

Heldmann, J.L., Toon, O.B., Pollard, W.H., Mellon, M.T., Pitlick, J., McKay, C.P., Andersen, D.T., 2005. Formation of martian gullies by the action of liquid water flowing under current martian environmental conditions. J. Geophys. Res. 110, doi:10.1029/2004JE002261.

Hellman, M.J., Ramsey, M.S., 2004. Analysis of hot springs and associated deposits in Yellowstone National Park using ASTER and AVIRIS remote sensing. J. Volcan. Geotherm. Res. 135, 195–219.

Herkenhoff, K.E., and 32 colleagues, 2004. Evidence from Opportunity's microscopic imager for water on Meridiani Planum. Science 306, 1727–1730.

Hoefen, T.M., Clark, R.N., Bandfield, J.L., Smith, M.D., Pearl, J.C., Christensen, P.R., 2003. Discovery of olivine in the Nili Fossae region of Mars. Science 302, 627–630.

Houtkooper, J.M., Schulze-Makuch, D., 2007. A possible biogenic origin for hydrogen peroxide on Mars: The Viking results reinterpreted. Int. J. Astrobiol., in press.

Hynek, B.M., 2004. Implications for hydrologic processes on Mars from extensive bedrock outcrops throughout Terra Meridiani. Nature 431, 156–159.

Hynek, B.M., Arvidson, R.E., Phillips, R.J., 2002. Geologic setting and origin of Terra Meridiani hematite deposit on Mars. J. Geophys. Res. 107, doi:10.1029/2002JE001891. 5088.

Jaumann, R., Reiss, D., Sander, T., Gwinner, K., Roatsch, T., Matz, K.-D., Hauber, E., Mertens, V., Hoffmann, H., Neukum, G., 2006. Source regions and water release mechanisms of martian valley networks. In: Europlanet Conference, 18–22 Sept. 2006, Berlin, Germany. Abstract A-00034.

Keller, J.M., and 17 colleagues, 2006. Equatorial and midlatitude distribution of chlorine measured by Mars Odyssey GRS. J. Geophys. Res. 111, doi:10.1029/2006JE002679. E03S08.

Keszthelyi, L., McEwen, A.S., Thordarson, T.H., 2000. Terrestrial analogs and thermal models for martian flood lavas. J. Geophys. Res. 105, 15027–15050.

Knauth, L.P., Burt, D.M., Wohletz, K.H., 2005. Impact origin of sediments at the Opportunity landing site on Mars. Nature 438, 1123–1128.

Komatsu, G., Dohm, J.M., Hare, T.M., 2004a. Hydrogeologic processes of large-scale tectonomagmatic complexes in Mongolia–southern Siberia and on Mars. Geology 32, 325–328.

Komatsu, G., Ori, G.G., Ciarcelluti, P., Litasov, Y., 2004b. Interior layered deposits of Valles Marineris, Mars: Analogous subice volcanism related to Baikal rifting, Southern Siberia. Planet. Space Sci. 52, 167–187.

Kring, D.A., 2000. Impact events and their effect on the origin, evolution, and distribution of life. GSA Today 10, 1–7.

Kuzmin R.O., Greeley, R., Landheim, R., Cabrol, N.A., Farmer, J.D., 2004. Geologic map of the MTM-15182 and MTM-15187 quadrangles, Gusev crater Ma'adim Vallis region, Mars. USGS Map I-2666.

Lanagan, P.D., McEwen, A.S., Keszthelyi, L.P., Thordarson, Th., 2001. Rootless cones on Mars indicating the presence of shallow equatorial ground ice in recent times. Geophys. Res. Lett. 28 (12), 2365–2367.

Lane, M.D., Morris, R.V., Mertzman, S.A., Christensen, P.R., 1999. Evidence for platy hematite grains in Sinus Meridiani, Mars. J. Geophys. Res. 107 (E12). 5126.

Langevin, Y., Poulet, F., Bibring, J.-P., Goudet, B., 2005. Sulfates in the north polar region of Mars detected by Omega/Mars Express. Science 307, 1584–1586.

Lee, P., 2002. Mars on Earth: The NASA Haughton-Mars project. Ad Astra: Mag. Nat. Space Soc., 12–52.

Leistel, J.M., Marcoux, E., Thiéblemont, D., Quesada, C., Sánchez, A., Almodovar, G.R., Pascual, E., Sáez, R., 1998. The volcanic-hosted massive sulfidic deposits of the Iberian Pyritic Belt. Miner. Deposita 33, 2–30.

Li, Z.X., Li, X.H., Kinny, P.D., Wang, J., Zhang, S., Zhou, H., 2003. Geochronology of Neoproterozoic syn-rift magmatism in the Yangtze Craton, South China and correlations with other continents: Evidence for a mantle superplume that broke up Rodinia. Precambrian Res. 122, 85–109.

Lucchitta, B.K., 1987. Recent mafic volcanism on Mars. Science 235, 565–567.

Lucchitta, B.K., Clow, G.D., Geissler, P.E., McEwen, A.S., Schultz, R.A., Singer, R.B., Squyres, S.W., 1992. The canyon system on Mars. In: Kieffer, H.H., Jakosky, B.M., Snyder, C.W., Matthews, M.S. (Eds.), Mars. Univ. of Arizona Press, Tucson, pp. 453–492.

MacKinnon, D.J., Tanaka, K.L., 1989. The impacted martian crust: Structure, hydrology, and some geologic implications. J. Geophys. Res. 94, 17359–17370.

Mangold, N., Quantin, C., Ansan, V., Delacourt, C., Allemand, P., 2004. Evidence for precipitation on Mars from dendritic valleys in the Valles Marineris area. Science 305, 78–81.

Maillaux, B.J., Person, M., Kelley, S., Dunbar, N., Cather, S., Strayer, L., Hudleton, P., 1999. Tectonic controls on the hydrogeology of the Rio Grande Rift, New Mexico. Water Resour. Res. 35, 2641–2660.

Malin, M.C., Edgett, K.S., Posiolova, L.V., McColley, S.M., Dobrea, E.Z.N., 2006. Present-day impact cratering rate and contemporary gully activity on Mars. Science 314, 1573–1577.

Maruyama, S., 1994. Plume tectonics. J. Geol. Soc. Jpn. 100, 24–49.

McCarville, P., Crossey, L.J., 1996. Post-impact hydrothermal alteration of the Manson Impact Structure, Manson, Iowa. In: Koeberl, C., Anderson, R. (Eds.), The Manson Impact Structure, Iowa: Anatomy of an Impact Crater. GSA Special Paper 302, pp. 347–376.

McKay, C.P., Stoker, C.R., 1989. The early environment and its evolution on Mars: Implications for life. Rev. Geophys. 27, 189–214.

McKee, E.D., 1966. Structures of dunes at White Sands National Monument, New Mexico (and a comparison with structures of dunes from other selected areas). Sedimentology 7, 3–69.

McKee, E.D., Moiola, R.J., 1975. Geometry and growth of the White Sands dune field, New Mexico. J. Res. US Geol. Surv. 3, 59–66.

Melosh, H.J., 1988. The rocky road to panspermia. Nature 332, 687–688.

Mojzsis, S.J., Harrison, T.M., 2000. Vestiges of a beginning: Clues to the emergent biosphere recorded in the oldest known sedimentary rocks. GSA Today 10, 1–6.
Mitchell, D.L., Lillis, R.J., Lin, R.P., Connerney, J.E.P., Acuna, M.H., 2007. A global map of Mars' crustal magnetic field based on electron reflectometry. J. Geophys. Res. 112, doi:10.1029/2005JE002564. E01002.
Moore, H.J., 2001. Geologic map of the Tempe–Mareotis region of Mars. US Geological Survey Geologic Investigations Series I-2727, scale 1:1,000,000.
Moore, J.M., Wilhelms, D.E., 2001. Hellas as a possible site of ancient ice-covered lakes on Mars. Icarus 154, 258–276.
Morris, E.C., Tanaka, K.L., 1994. Geologic map of the Olympus Mons region of Mars. USGS Misc. Inv. Ser. Map I-2327.
Mouginis-Mark, P.J., Wilson, L., Head, J.W., Brown, S.H., Hall, J.L., Sullivan, K.D., 1984. Elysium Planitia, Mars: Regional geology, volcanology, and evidence for volcano–ground ice interactions. Earth Moon Planets 30, 149–173.
Mouginis-Mark, P.J., 1985. Volcano/ground ice interactions in Elysium Planitia, Mars. Icarus 64, 265–284.
Mouginis-Mark, P.J., 1990. Recent water release in the Tharsis region of Mars. Icarus 84, 362–373.
Murray, J.B., Muller, J., Neukum, G., Hauber, E., Markiewicz, W.J., Head III, J.W., Foing, B.H., Page, D., Mitchell, K.L., Portyankina, G., and the HRSC co-investigator Team, 2005. Evidence from the Mars Express High Resolution Stereo Camera for a frozen sea close to the Mars equator. Nature 434, 352–356.
Mustard, J.F., Poulet, F., Mangold, N., Bibring, J.-P., Milliken, R.E., Pelkey, S., 2006. Aqueous alteration and evidence of habitability in Nili Fossae. In: First Landing Site Workshop for the 2009 Mars Science Laboratory, May 31–June 2, 2006, Pasadena, CA. Abstract.
Naumov, M.V., 2002. Impact-generated hydrothermal systems: Data from Popigai, Kara, and Puchezh–Katunki impact structures in impacts in Precambrian shield. In: Plado, J., Pesonen, L.J. (Eds.), Impacts in Precambrian Shields. Springer-Verlag, Berlin, pp. 117–171.
Neukum, G., van Gasselt, S., 2006. Recent volcanism at the martian north pole. Geophys. Res. Abstracts 8, 11103.
Newell, D.L., Crossey, L.J., Karlstrom, K., Fischer, T., Hilton, D., 2005. Evidence for continental-scale links between the mantle and groundwater systems of the western United States based on hydrochemistry of travertine-depositing springs and regional synthesis of helium isotopic data. GSA Today 15, 4–10.
Newsom, H.E., 1980. Hydrothermal alteration of impact melt sheets with implications for Mars. Icarus 44, 207–216.
Newsom, H.E., Brittelle, G.E., Hibbitts, C.A., Crossey, L.J., Kudo, A.M., 1996. Impact crater lakes on Mars. J. Geophys. Res. 101, 14951–14955.
Newsom, H.E., Nelson, M.J., Shearer, C.K., Misra, S., 2003. Hydrothermal processes in impact craters on Mars: Implications from Lonar Crater, India, and other craters. In: American Geophysical Union, Fall Meeting 2004. Abstract P34A-06.
Osinski, G.R., Spray, J.G., Lee, P., 2001. Impact-induced hydrothermal activity within the Haughton impact structure, arctic Canada: Generation of a transient, warm, wet oasis. Meteor. Planet. Sci. 36, 731–745.
Osinski, G.R., Lee, P., Parnell, J., Spray, J.G., Baron, M., 2005. A case study of impact induced hydrothermal activity: The Haughton impact structure, Devon Island, Canadian High Arctic. Meteor. Planet. Sci. 40, 1859–1877.
Page, D., Murray, J.B., 2006. Stratigraphical and morphological evidence for pingo genesis in the Cerberus plains. Icarus 183, 46–54.
Pevzner, L.A., Kirjakov, A.F., Vorontsov, A.K., Masaitis, V.L., Mashchak, M.S., Ivanov, B.A., 1992. Vorotilovskaya drillhole: First deep drilling in the central uplift of large terrestrial impact crater. Lunar Planet. Sci. XXIII, 1063–1064.
Pieri, D.C., 1976. Distribution of small channels on the martian surface. Icarus 27, 25–50.
Plescia, J.B., 1990. Recent flood lavas in the Elysium region of Mars. Icarus 88, 465–490.
Plescia, J.B., 2003. Cerberus Fossae, Elysium, Mars: A source for lava and water. Icarus 164, 79–95.
Plescia, J.B., 2005. Acheron Fossae, Mars: Evidence of fluvial activity and mass flow. Lunar Planet. Sci. XXXVII. Abstract 1488.
Rathbun, J.A., Squyres, S.W., 2002. Hydrothermal systems associated with martian impact craters. Icarus 157, 362–372.
Reiss, D., Jaumann, R., 2002. Recent debris flows on Mars: Seasonal observations of the Russell Crater dune field. Geophys. Res. Lett. 30. 1321.
Reiss, D., Stephan, K., van Gesselt, S., Hauber, E., Jaumann, R., Neukum, G., 2004. Regional differences in gully occurrence on Mars: A comparison between Hale and Bond craters using HRSC, THEMIS-IR and MOC Data. In: American Geophysical Union, Fall Meeting 2004. Abstract P34A-05.
Rieder, R., and 14 colleagues, 2004. Chemistry of rocks and soils at Meridiani Planum from the alpha particle X-ray spectrometer. Science 306, 1746–1749.
Robinson, M.S., Mouginis-Mark, P.J., Zimbelman, J.R., Wu, S.S.C., Ablin, K.K., Howington-Kraus, A.E., 1993. Chronology, eruption duration, and atmospheric contribution of the martian volcano, Apollinaris Patera. Icarus 104, 301–323.
Rodriguez, J.A.P., Sasaki, S., Kuzmin, R.O., Dohm, J.M., Tanaka, K.L., Miyamoto, H., Kurita, K., Komatsu, G., Fairen, A.G., Ferris, J.C., 2005a. Outflow channel sources, reactivation, and chaos formation, Xanthe Terra, Mars. Icarus 175, 36–57.
Rodriguez, J.A., and 12 colleagues, 2005b. Control of impact crater fracture systems on subsurface hydrology, ground subsidence, and collapse, Mars. J. Geophys. Res. 110, doi:10.1029/2004JE002365.
Ruff, S.W., Christensen, P.R., Clark, R.N., Kieffer, H.H., Malin, M.C., Bandfield, J.L., Jakosky, B.M., Lane, M.D., Mellon, M.T., Presley, M.A., 2001. Mars' "White Rock" feature lacks evidence of an aqueous origin: Results from Mars Global Surveyor. J. Geophys. Res. 106 (E10), 23921–23928.
Russell, M.J., Sunar, F., Hall, A.J., Fallick, A.E., Ingham, J.K., Zedef, V., Maktav, D., 1999. Search for signs of ancient life on Mars: Expectations from hydromagnesite microbialites, Salda Lake, Turkey. J. Geol. Soc. 156, 869–888.
Rzonca, B., Schulze-Makuch, D., 2003. Correlation between microbial and chemical parameters of some hydrothermal springs in New Mexico, USA. J. Hydrol. 280, 272–284.
Sass, J.H., Morgan, P., 1988. Conductive heat flux in VC-1 and the thermal regime of Valles Caldera, Jemez Mountains, New Mexico. J. Geophys. Res. 93, 6027–6039.
Schenk, C.J., Fryberger, S.G., 1988. Early diagenesis of eolian dune and interdune sands at White Sands, New Mexico. Sediment. Geol. 55, 109–120.
Schubert, G., Solomon, S.C., Turcotte, D.L., Drake, M.J., Sleep, N.H., 1992. Origin and thermal evolution of Mars. In: Kieffer, H.H., Jakosky, B.M., Snyder, C.W., Matthews, M.S. (Eds.), Mars. Univ. of Arizona Press, Tucson, pp. 147–183.
Schultz, R.A., Tanaka, K.L., 1994. Lithospheric-scale buckling and thrust structures on Mars: The Coprates rise and south Tharsis ridge belt. J. Geophys. Res. 99, 8371–8385.
Schulze-Makuch, D., 2002. Evidence for the discharge of hydrothermal water into Lake Lucero, White Sands National Monument, Southern New Mexico. In: New Mexico Geological Society Guidebook, 53rd Field Conference, Geology of White Sands, pp. 325–329.
Schulze-Makuch, D., Irwin, L.N., 2004. Life in the Universe: Expectations and Constraints. Springer-Verlag, Berlin.
Schulze-Makuch, D., Irwin, L.N., Lipps, J.H., LeMone, D., Dohm, J.M., Fairén, A.G., 2005a. Scenarios for the evolution of life on Mars. J. Geophys. Res. 110, doi:10.1029/2005JE002430. E12S23. Special Edition on Early Mars.
Schulze-Makuch, D., Dohm, J.M., Fairén, A.G., Baker, V.R., Fink, W., Strom, R.G., 2005b. Venus, Mars, and the ices on Mercury and the Moon: Astrobiological implications and proposed mission designs. Astrobiology 5, 778–795.
Scott, D.H., Dohm, J.M., 1990. Faults and ridges—Historical development in Tempe Terra and ULYSSES Patera regions of Mars. Proc. Lunar Sci. Conf. XX, 503–513.
Scott, D.H., Tanaka, K.L., 1986. Geologic map of the western equatorial region of Mars, USGS Misc. Inv. Ser. Map I-1802-A (1:15,000,000).
Scott, D.H., Zimbelman, J.R., 1995. Geologic map of Arsia Mons volcano, Mars. Geo. Invest. Series Map I-2480, scale 1:1,000,000, USGS.
Scott, D.H., Dohm, J.M., Applebee, D.J., 1993. Geologic map of science study area 8, Apollinaris Patera region of Mars. USGS Misc. Inv. Ser. Map I-2351 (1:500,000).

Scott, D.H., Dohm, J.M., Rice Jr., J.W., 1995. Map of Mars showing channels and possible paleolake basins. USGS Misc. Inv. Ser. Map I-2461 (1:30,000,000).

Segura, T.L., Toon, O.B., Colaprete, A., Zahnle, K., 2002. Environmental effects of large impacts on Mars. Science 298, 1977–1980.

Shean, D.E., Head, J.W., Marchant, D.R., 2005. Origin and evolution of a cold-based tropical mountain glacier on Mars: The Pavonis Mons fan-shaped deposit. J. Geophys. Res. 110, doi:10.1029/2004JE002360.

Shuster, D.L., Weiss, B.P., 2005. Martian surface paleotemperatures from thermochronology of meteorites. Science 309, 594–600.

Simonds, C.H., McGee, P.E., 1979. Petrology of impactites from lake St. Martin structure, Manitoba. Proc. Lunar Sci. Conf. XX, 2493–2518.

Squyres, S.W., Wilhelms, D.E., Moosman, A.C., 1987. Large-scale volcano–ground ice interactions on Mars. Icarus 70, 385–408.

Squyres, S.W., and 18 colleagues, 2004. In situ evidence for an ancient aqueous environment at Meridiani Planum, Mars. Science 306, 1709–1714.

Strom, R.G., Malhotra, R., Ito, T., Yoshida, F., Kring, D.A., 2005. The origin of planetary impactors in the inner Solar System. Science 309, 1847–1850.

Tanaka, K.L., 1986. The stratigraphy of Mars. In: Proc. Lunar Sci. Conf. XVII, Part 1. J. Geophys. Res. 91, E139–E158.

Tanaka, K.L., Scott, D.H., 1987. Geologic map of the polar regions of Mars, USGS Misc. Inv. Ser. Map I-1802-c (1:15,000,000).

Tanaka, K.L., Scott, D.H., Greeley, R., 1992. Global stratigraphy. In: Kieffer, H.H., Jakosky, B.M., Snyder, C.W., Matthews, M.S. (Eds.), Mars. Univ. of Arizona Press, Tucson, pp. 818–834.

Tanaka, K.L., Dohm, J.M., Lias, J.H., Hare, T.M., 1998. Erosional valleys in the Thaumasia region of Mars: Hydrothermal and seismic origins. J. Geophys. Res. 103, 31407–31419.

Tanaka, K.L., Kargel, J.S., MacKinnon, D.J., Hare, T.M., Hoffman, N., 2002. Catastrophic erosion of Hellas basin rim on Mars induced by magmatic intrusion into volatile-rich rocks, Geophys. Res. Lett. 29, doi:10.1029/2001GL013885.

Tanaka, K.L., Skinner, J.A., Hare, T.M., Joyal, T., Wenker, A., 2003. Resurfacing history of the northern plains of Mars based on geologic mapping of Mars Global Surveyor data. J. Geophys. Res. 108, doi:10.1029/2002JE001908.

Tanaka, K.L., Skinner Jr., J.A., Hare, T.M., 2005. Geologic map of the northern plains of Mars. US Geological Survey Scientific Investigations Map SIM-2888, scale 1:15,000,000.

Taylor, G.J., and 26 colleagues, 2006. Variations in K/Th on Mars. J. Geophys. Res. 111, doi:10.1029/2006JE002676. E03S06.

Tera, F., Papanastassiou, D.A., Wasserburg, G.J., 1974. Isotopic evidence for a terminal lunar cataclysm. Earth Planet. Sci. Lett. 22, 1–21.

Thorsos, I.E., Newsom, H.E., Davies, A.G., 2001. Availability of heat to drive hydrothermal systems in large martian impact craters. Lunar Planet. Sci. XXXII. Abstract 2011.

Truesdell, A.H., Janik, C.J., 1986. Reservoir processes and fluid origins in the Baca geothermal system, Valles Caldera, New Mexico. J. Geophys. Res. 91, 1817–1834.

Williams, S.H., Zimbelman, J.R., 1994. "White Rock": An eroded martian lacustrine deposit (?). Geology 22, 107–110.

Wilson, L., Head, J.W., 1997. Mars geothermal and volcanic evolution: Volcanic intrusions as heat sources to maintain viable ecosystems? In: Conference on Early Mars: Geologic and Hydrologic Evolution, Physical and Chemical Environments, and the Implications for Life, LPI Contribution 96, 85–87.

Witbeck, N.E., Tanaka, K.L., Scott, D.H., 1991. US Geol. Surv. Misc. Invest. Serv. Map I-2010.

Zurcher, L., Kring, D.A., 2004. Hydrothermal alteration in the Yaxcopoil-1 borehole, Chicxulub impact structure, Mexico. Meteor. Planet. Sci. 39, 1199–1222.